

Dispersive regime of multiphoton qubit-oscillator interactions

Mohammad Ayyash^{1,2,*} and Sahel Ashhab³

¹*Red Blue Quantum Inc., 72 Ellis Crescent North, Waterloo, Ontario N2J 3N8, Canada*

²*Institute for Quantum Computing, University of Waterloo,*

200 University Avenue West, Waterloo, Ontario N2L 3G1, Canada

³*Advanced ICT Research Institute, National Institute of Information and Communications Technology,
4-2-1, Nukui-Kitamachi, Koganei, Tokyo 184-8795, Japan*

(Dated: March 28, 2025)

The dispersive regime of n -photon qubit-oscillator interactions is analyzed using Schrieffer-Wolff perturbation theory. Effective Hamiltonians are derived up to the second order in the perturbation parameters. These effective descriptions reveal higher-order qubit-oscillator cross-Kerr and oscillator self-Kerr terms. The cross-Kerr term combines a qubit Pauli operator with an n -degree polynomial in the oscillator photon number operator, while the self-Kerr term is an $(n-1)$ -degree polynomial in the oscillator photon number operator. In addition to the higher-order Kerr terms, a qubit-conditional $2n$ -photon squeezing term appears in the effective non-rotating-wave-approximation Hamiltonian. Furthermore, perturbation theory is applied to the case of multiple qubits coupled to a shared oscillator. A photon-number-dependent qubit-qubit interaction emerges in this case, which can be leveraged to tune the effective multiqubit system parameters using the oscillator state. Results for the converse setup of multiple oscillators and a single qubit are also derived. In this case, a qubit-conditional oscillator-oscillator nonlinear interaction is found. The effective descriptions developed here offer a simple and intuitive physical picture of dispersive multiphoton qubit-oscillator interactions that can aid in the design of implementations harnessing their desired nonlinear effects.

I. INTRODUCTION

The simplest picture of a quantum-mechanical light-matter interaction is captured by a single qubit coupled to a single harmonic oscillator. The prototypical model is known as the (quantum) Rabi model and was first introduced by Jaynes and Cummings in 1963 [1] as a quantum-mechanical generalization of the pioneering semiclassical model formulated in 1936 by Rabi [2, 3]. Jaynes and Cummings simplified the Rabi model to the widely-used model that now bears their names, the Jaynes-Cummings (JC) model, which has a closed-form solution and applies under the rotating-wave-approximation (RWA) where the counter-rotating and energy-non-conserving terms are neglected. These qubit-oscillator models form the theoretical underpinning of various disciplines in quantum physics such as cavity quantum electrodynamics (QED) [4], circuit QED [5] and trapped ions [6].

The qubit-oscillator interaction described in the Rabi and JC models is one of a linear nature where single photons (or, more generally, excitations) are created and annihilated in the oscillator. Generalizations were later formulated with the qubit-oscillator interactions being intensity or photon-number dependent [7–9]. Additionally, multiphoton generalizations were proposed where more than one photon is created or annihilated in each emission or absorption event [7, 10–12]. For a review on various generalizations of the Rabi model, see Ref.[13] and references therein.

The aforementioned studies spurred an active area of research focused on the spectral and dynamical features

of the generalized Rabi and JC models. One particularly peculiar phenomenon occurs in some variants of the n -photon Rabi models; the feature known as the “spectral collapse” where the joint qubit-oscillator spectra and eigenstates transition from a discretely indexed set to a degenerate continuum above a critical qubit-oscillator coupling strength [14, 15]. For the two-photon Rabi model, a quasi-analytical solution was found in the studies of Refs. [16, 17] based on the same method used by Braak [18] to solve the one-photon case. Other works used generalized Bogoliubov transformations to arrive at the same solution [19, 20]. In parallel with the spectral and analytical studies of multiphoton models, there have been a number of quantum information applications developed that leverage nonlinear qubit-oscillator interactions [21–23]. Experimentally feasible implementations were proposed for superconducting circuits [22, 24–26] and trapped ions [21, 27], and very recently, qubit-conditional n -photon squeezing for $n = 2, 3, 4$ was experimentally realized in a trapped ions setup [23].

In this paper, we aim to add more insight to the study of multiphoton qubit-oscillator interactions. While quasi-analytical solutions for the two-photon Rabi model were found [16, 17, 19, 20], they lack an intuitive and physically-motivated picture. We seek to uncover a more intuitive picture than the rigorous mathematical solutions of the spectra of n -photon qubit-oscillator models in the dispersive regime, where the qubit-oscillator n -photon coupling is much smaller than the n -photon qubit-oscillator detuning as we will define later. We resort to second-order Schrieffer-Wolff (SW) perturbation theory to obtain analytic expressions for the qubit-oscillator spectra in the dispersive regime by generalizing techniques employed with the Rabi and JC models

* mmayyash@uwaterloo.ca

[28–30]. We then consider two further multipartite generalizations of this multiphoton dispersive perturbation theory; the case of many qubits nonlinearly coupled to a shared oscillator and the converse case of many oscillators nonlinearly coupled to a shared qubit.

The paper is structured as follows. In Sec. II, we review relevant previous work. In particular, we recall the typically used SW perturbation theory for the dispersive regime of linear qubit-oscillator interactions that we seek to generalize. Section III defines the multiphoton dispersive regime and lays out the generalized SW transformations for the RWA and non-RWA regimes. The analytically-obtained spectra are compared to numerical results to establish a regime of validity. The transformations are then used in the multiqubit-single-oscillator scenario in Sec. IV. The multioscillator-single-qubit converse case is discussed in Sec. V. The results are summarized and conclusions are given in Sec. VI. Appendix A outlines the details of the combinatorics and commutators used in the SW perturbation theory developed in the main text.

II. BACKGROUND

In this section, we briefly introduce the Rabi model and its subsequent approximations and relevant generalizations that are instrumental for the results to be presented. We begin with models relying on linear interactions in the case of a single qubit-oscillator system followed by the multipartite cases of many qubits linearly coupled to a single oscillator and many oscillators linearly coupled to a single qubit. In each case, we derive an effective RWA and non-RWA dispersive Hamiltonian using second-order perturbation theory. Finally, we introduce the multiphoton generalized models of interest for which we seek to develop a similar perturbation theory for the RWA and non-RWA n -photon dispersive regimes.

A. Single qubit-oscillator system

The Hamiltonian of the Rabi model reads ($\hbar = 1$)

$$\hat{H}_R = \omega_o \hat{a}^\dagger \hat{a} + \frac{\omega_q}{2} \hat{\sigma}_z + g \hat{\sigma}_x (\hat{a}^\dagger + \hat{a}), \quad (1)$$

where ω_q is the qubit transition frequency, ω_o is the oscillator resonance frequency and g is the qubit-oscillator coupling strength. Here, $\hat{\sigma}_z = |e\rangle\langle e| - |g\rangle\langle g|$ describes the population difference between the qubit's ground, $|g\rangle$, and excited, $|e\rangle$, states, $\hat{\sigma}_x = \hat{\sigma}_+ + \hat{\sigma}_-$ is the dipole operator with $\hat{\sigma}_+ = |e\rangle\langle g|$ and $\hat{\sigma}_- = \hat{\sigma}_+^\dagger$, and \hat{a}^\dagger and \hat{a} are the oscillator's creation and annihilation operators obeying $[\hat{a}, \hat{a}^\dagger] = \hat{1}$. When the coupling strength and qubit and oscillator frequencies satisfy

$$|\Delta| \ll \Sigma \text{ and } g \ll \min(\omega_q, \omega_o) \quad (2)$$

with $\Delta = \omega_q - \omega_o$ and $\Sigma = \omega_q + \omega_o$, the Hamiltonian of Eq. (1) can be simplified using an RWA to read as

$$\hat{H}_R \simeq \hat{H}_{JC} = \omega_o \hat{a}^\dagger \hat{a} + \frac{\omega_q}{2} \hat{\sigma}_z + g(\hat{\sigma}_+ \hat{a} + \hat{\sigma}_- \hat{a}^\dagger). \quad (3)$$

The spectra and eigenstates of the JC Hamiltonian are exactly solvable. Within the JC regime of validity defined in Eq. (2) lies the dispersive regime where

$$g \ll |\Delta| \ll \Sigma. \quad (4)$$

In the dispersive regime, the JC eigenstates are well approximated by the bare states of $\hat{H}_0 = \omega_o \hat{a}^\dagger \hat{a} + \omega_q \hat{\sigma}_z/2$, $\{|g, n\rangle, |e, n\rangle\}$, and, as such, the JC interaction term can be treated as a perturbation. Thus, it is helpful to apply a SW transformation [31] that perturbatively diagonalizes the Hamiltonian in the bare basis. The transformation is defined as [4, 28]

$$\hat{U}_{\text{Disp,RWA}} = \exp(\lambda \hat{X}_-), \quad (5a)$$

where

$$\lambda = \frac{g}{\Delta} \quad (5b)$$

and

$$\hat{X}_\pm = \hat{\sigma}_- \hat{a}^\dagger \pm \hat{\sigma}_+ \hat{a}. \quad (5c)$$

The interaction term in the JC model corresponds to $g\hat{X}_+$. Then, we transform the Hamiltonian using this unitary operator and expand using the Baker-Campbell-Hausdorff (BCH) identity, up to second order in λ , to obtain the dispersive RWA Hamiltonian

$$\begin{aligned} \hat{H}_{\text{Disp,RWA}} &= \hat{U}_{\text{Disp,RWA}}^\dagger \hat{H}_{JC} \hat{U}_{\text{Disp,RWA}} \\ &\simeq \omega_o \hat{a}^\dagger \hat{a} + \frac{\omega_q}{2} \hat{\sigma}_z + \chi \hat{\sigma}_z \left(\frac{1}{2} + \hat{a}^\dagger \hat{a} \right), \end{aligned} \quad (6)$$

where $\chi = g^2/\Delta$ is the dispersive shift. Here, we employ second-order SW perturbation theory since the first-order term in the BCH expansion, $\lambda[\hat{H}_{JC}, \hat{X}_-]$, yields terms quadratic in λ , and the second-order term, $\lambda^2[[\hat{H}_{JC}, \hat{X}_-], \hat{X}_-]/2!$, leads to terms that are quadratic and quartic in λ . Thus, we need to go to second order in SW perturbation theory to account for all the terms that are quadratic in λ . This will be the case for all perturbative expansions in this paper. This Hamiltonian is typically employed for quantum-nondemolition measurements of a qubit using an oscillator. The perturbative second-order expansion is typically considered valid when $\lambda \ll 1$. However, strictly speaking, there is an additional constraint; the oscillator average occupation must remain lower than the critical photon number $n_c = \lambda^2/4 = g^2/4\Delta^2$. Thus, the approximate description becomes less accurate for larger λ and/or higher oscillator photon occupation. In either of these cases, higher-order corrections in the expansion are required [28]. The

critical photon number places a bound on the linear dispersive regime where the oscillator does not exhibit any nonlinearity, e.g. $(\hat{a}^\dagger \hat{a})^2$, as it would from higher-order corrections. There have been works studying the higher-order corrections and the effect of the qubit-induced oscillator nonlinearity on the efficacy of qubit readout [32].

Due to the accessible strong nonlinearities in circuit QED implementations, it became possible to reach the ultrastrong coupling regime where the hierarchy of energy scales in Eq. (2) no longer holds. In the ultrastrong coupling regime, the effects of counter-rotating terms neglected from Eq. (1) become considerable and have been experimentally verified [33–35]. It is then possible to be simultaneously in the dispersive and ultrastrong coupling regimes where $|\Delta| \ll \Sigma$ in Eq. (4) is no longer necessarily true. We refer to this as the non-RWA dispersive regime [29]. This defines a hierarchy where the non-RWA dispersive regime contains its RWA counterpart within it. When the RWA no longer applies, we need to extend the SW transformation of Eq. (5) to account for the counter-rotating terms present in Eq. (1). The new transformation reads [29]

$$\hat{U}_{\text{Disp}} = \exp\left(\lambda \hat{X}_- + \bar{\lambda} \hat{Y}_-\right), \quad (7a)$$

where

$$\bar{\lambda} = \frac{g}{\Sigma} \quad (7b)$$

and

$$\hat{Y}_\pm = \hat{\sigma}_- \hat{a} \pm \hat{\sigma}_+ \hat{a}^\dagger. \quad (7c)$$

Note that \hat{Y}_\pm and \hat{X}_\pm do not commute. In the Rabi model, the interaction part can be expressed as $g(\hat{X}_+ + \hat{Y}_+)$. Applying the same procedure of transforming the Hamiltonian and using the BCH expansion to second order in both λ and $\bar{\lambda}$, we obtain the non-RWA dispersive Hamiltonian

$$\begin{aligned} \hat{H}_{\text{Disp}} &= \hat{U}_{\text{Disp}}^\dagger \hat{H}_{\text{R}} \hat{U}_{\text{Disp}} \\ &\simeq \omega_o \hat{a}^\dagger \hat{a} + \frac{\omega_q}{2} \hat{\sigma}_z + (\chi + \xi) \hat{\sigma}_z \left(\frac{1}{2} + \hat{a}^\dagger \hat{a} \right) \\ &\quad + \frac{(\chi + \xi)}{2} \hat{\sigma}_z (\hat{a}^{\dagger 2} + \hat{a}^2), \end{aligned} \quad (8)$$

where $\xi = g^2/\Sigma$ is the Bloch-Siegert shift coefficient. Note that the last two terms in the Hamiltonian can be combined into one term, $(\chi + \xi) \hat{\sigma}_z (\hat{a}^\dagger + \hat{a})^2/2$. However, we choose to keep these terms separated since the generalized multiphoton we present later are in the same form. Interestingly, the non-RWA dispersive Hamiltonian exhibits qubit-conditional squeezing. This resulting interaction was proposed as a mechanism for generating squeezed states in the oscillator [36].

It is worth noting that one can absorb the qubit-conditional squeezing into the transformation by introducing an appropriate generator in the non-RWA

Schrieffer-Wolff transformation of Eq. (7). This ensures that the Hamiltonian is diagonal in its bare basis which is not the case in the presence of $\hat{\sigma}_z (\hat{a}^{\dagger 2} + \hat{a}^2)$. The new transformation reads [30]

$$\hat{\tilde{U}}_{\text{Disp}} = \exp\left(\lambda \hat{X}_- + \bar{\lambda} \hat{Y}_- + \zeta \hat{Z}\right), \quad (9a)$$

where

$$\zeta = \frac{g\bar{\lambda}}{2\omega_o} \quad (9b)$$

and

$$\hat{Z} = \hat{\sigma}_z (\hat{a}^2 - \hat{a}^{\dagger 2}). \quad (9c)$$

Then, using this transformation, we obtain a diagonal non-RWA dispersive Hamiltonian in the bare basis up to second order in all perturbation parameters.

B. Multiple qubits coupled to a single oscillator

We now turn our attention to the case of multiple qubits linearly coupled to a single oscillator known as the Dicke model [37]. The Dicke Hamiltonian is

$$\begin{aligned} \hat{H}_{\text{D}}^N &= \omega_o \hat{a}^\dagger \hat{a} + \sum_{l=1}^N \frac{\omega_q^{(l)}}{2} \hat{\sigma}_z^{(l)} \\ &\quad + \sum_{l=1}^N g^{(l)} \hat{\sigma}_x^{(l)} (\hat{a}^\dagger + \hat{a}), \end{aligned} \quad (10)$$

where the superscript (l) signifies the l th qubit. The origins of this model lie in the pioneering work of Dicke on superradiance in ensembles of two-level atoms [37]. However, the above form of this model was used in the study of superradiant phase transitions of a radiation field mode coupled to an ensemble of two-level systems past a critical coupling strength [38, 39].

When the qubits are individually in the JC-RWA regime defined by Eq. (2), i.e. $|\Delta^{(l)}| \ll \Sigma^{(l)}$ and $g^{(l)} \ll \min(\omega_q^{(l)}, \omega_o)$ holds for all $\omega_q^{(l)}$ and $g^{(l)}$ with $\Delta^{(j)} = \omega_q^{(j)} - \omega_o$ and $\Sigma^{(j)} = \omega_q^{(j)} + \omega_o$, the counter-rotating terms can be neglected to obtain the Tavis-Cummings (TC) Hamiltonian [40]

$$\begin{aligned} \hat{H}_{\text{D}}^N &\simeq \hat{H}_{\text{TC}}^N = \omega_o \hat{a}^\dagger \hat{a} + \sum_{l=1}^N \frac{\omega_q^{(l)}}{2} \hat{\sigma}_z^{(l)} \\ &\quad + \sum_{l=1}^N g^{(l)} (\hat{\sigma}_+^{(l)} \hat{a} + \hat{\sigma}_-^{(l)} \hat{a}^\dagger). \end{aligned} \quad (11)$$

Very much like the JC model, the TC model is exactly solvable and its spectra can be found analytically. This model serves as an important basis for many quantum computing implementations such as circuit QED

[28]. In such a scenario, the oscillator can mediate interactions between qubits that are not directly coupled to each other. This is typically performed in the dispersive regime where Eq. (4) holds for each qubit, i.e. $g^{(j)} \ll |\Delta^{(j)}| \ll \Sigma^{(j)}$. In such a regime, we can apply a multipartite SW transformation that straightforwardly follows from the single qubit-oscillator case. Following the same procedure as before, the multiqubit RWA dispersive Hamiltonian reads as [28]

$$\begin{aligned} \hat{H}_{\text{Disp,RWA}}^N &\simeq \omega_o \hat{a}^\dagger \hat{a} + \sum_{l=1}^N \frac{\omega_q^{(l)}}{2} \hat{\sigma}_z^{(l)} \\ &+ \sum_{l=1}^N \chi^{(l)} \hat{\sigma}_z^{(l)} \left(\frac{1}{2} + \hat{a}^\dagger \hat{a} \right) \\ &+ \sum_{k>l} \tilde{\chi}^{(l,m)} (\hat{\sigma}_+^{(l)} \hat{\sigma}_-^{(m)} + \hat{\sigma}_-^{(l)} \hat{\sigma}_+^{(m)}) \end{aligned} \quad (12)$$

where $\chi^{(l)} = (g^{(l)})^2 / |\Delta^{(l)}|$, and $\tilde{\chi}^{(l,m)} = g^{(l)} g^{(m)} \left(\frac{1}{\Delta^{(l)}} + \frac{1}{\Delta^{(m)}} \right)$. In this setup, the oscillator mediates a qubit-qubit interaction of the isotropic XY type which is an excitation-conserving interaction. This type of mediated interaction has already been extensively used for implementing two-qubit gates and state tomography. The collective qubit-induced dispersive shift on the oscillator's frequency has been experimentally observed with up to 4000 qubits coupled to a shared oscillator [41].

Naturally, as the qubits' coupling to the shared oscillator becomes stronger, the hierarchy of energy scales is different than that of the RWA regime. The new parameter regime is then defined by $g^{(j)} \ll |\Delta^{(j)}|$. Here, $|\Delta^{(j)}| \ll \Sigma^{(j)}$ is no longer necessarily true, and, once again, there is a hierarchy where the non-RWA dispersive regime contains within it the RWA dispersive regime. In this case, we may now perturbatively expand the Dicke Hamiltonian where the counter-rotating terms are included as we did for the Rabi Hamiltonian. Then, the multiqubit non-RWA dispersive Hamiltonian becomes [29]

$$\begin{aligned} \hat{H}_{\text{Disp}}^N &= \hat{U}_{\text{Disp}}^{N\dagger} \hat{H}_{\text{D}}^N \hat{U}_{\text{Disp}}^N \\ &\simeq \omega_o \hat{a}^\dagger \hat{a} + \sum_{l=1}^N \frac{\omega_q^{(l)}}{2} \hat{\sigma}_z^{(l)} \\ &+ \sum_{l=1}^N (\chi^{(l)} + \xi^{(l)}) \hat{\sigma}_z^{(l)} \left(\frac{1}{2} + \hat{a}^\dagger \hat{a} \right) \\ &+ \sum_{k>l} (\tilde{\chi}^{(l,m)} - \tilde{\xi}^{(l,m)}) (\hat{\sigma}_x^{(l)} \hat{\sigma}_x^{(m)}), \end{aligned} \quad (13)$$

where $\xi^{(l)} = (g^{(l)})^2 / \Sigma^{(l)}$, and $\tilde{\xi}^{(l,m)} = g^{(l)} g^{(m)} \left(\frac{1}{\Sigma^{(l)}} + \frac{1}{\Sigma^{(m)}} \right)$. The presence of the counter-rotating terms gives rise to an Ising-type mediated qubit-qubit interaction, $\hat{\sigma}_x^{(l)} \hat{\sigma}_x^{(m)}$, which is not excitation preserving.

C. Multiple oscillators coupled to a single qubit

We now briefly highlight the converse multipartite case where multiple oscillators are coupled to a shared qubit. In relation to the quantum computational applications of the multiqubit-oscillator models, the multioscillator-qubit models can be thought of as an alternative paradigm; the computational or logical qubits are bosonically encoded in the oscillator, and the physical qubit is used to control and readout the bosonic modes [42, 43].

We start with the multimode Rabi (MR) model and its Hamiltonian that reads

$$\begin{aligned} \hat{H}_{\text{MR}} &= \sum_k \omega_k \hat{a}_k^\dagger \hat{a}_k + \frac{\omega_q}{2} \hat{\sigma}_z \\ &+ \sum_k g_k \hat{\sigma}_x (\hat{a}_k^\dagger + \hat{a}_k), \end{aligned} \quad (14)$$

where we label each mode and its frequencies with a subscript k (contrasted with a superscript for the case of multiple qubits). It is worth noting that a transmission line resonator contains an infinite, or at least a large, number of modes, such that a qubit coupled to a transmission line resonator is one case of multiple oscillators coupled to a single qubit [44–46]. Similarly to the relation between the Dicke and TC model, when the oscillators are within the RWA regime of Eq. (2), we can simplify the MR model by neglecting the counter-rotating terms. Thus, we perform an RWA and obtain the multimode JC (MJC) Hamiltonian

$$\begin{aligned} \hat{H}_{\text{MJC}} &= \sum_k \omega_k \hat{a}_k^\dagger \hat{a}_k + \frac{\omega_q}{2} \hat{\sigma}_z \\ &+ \sum_k g_k (\hat{\sigma}_+ \hat{a}_k + \hat{\sigma}_- \hat{a}_k^\dagger), \end{aligned} \quad (15)$$

Now that we have explicitly derived the single qubit-oscillator and multiqubit-oscillator cases, we simply state the results for the different regimes, and the derivations follow exactly from the multiqubit case with the exception that it is now a multioscillator system. We do not redefine all the parameters, and instead, we assume the indices now run over the oscillators rather than the qubits. In the RWA regime, the multioscillator RWA dispersive regime Hamiltonian reads as

$$\begin{aligned} \hat{H}_{\text{Disp,RWA}}^{\text{MO}} &\simeq \sum_k \omega_k \hat{a}_k^\dagger \hat{a}_k + \frac{\omega_q}{2} \hat{\sigma}_z \\ &+ \sum_k \chi_k \hat{\sigma}_z \left(\frac{1}{2} + \hat{a}_k^\dagger \hat{a}_k \right) \\ &+ \sum_{j>k} \frac{\tilde{\chi}_{j,k}}{2} \hat{\sigma}_z (\hat{a}_j^\dagger \hat{a}_k + \hat{a}_j \hat{a}_k^\dagger). \end{aligned} \quad (16)$$

Here, a qubit-conditional oscillator-oscillator beamsplitter interaction emerges between the uncoupled oscillators. This type of interaction has been leveraged for creating nonclassical states entangled between the oscillators and more generally, for implementing gates

for bosonic encodings [47, 48]. As expected, in the RWA regimes where the counter-rotating terms are neglected, the qubit-mediated oscillator interaction is of the excitation-conserving type (beamsplitter interaction). Similarly to the previous section, we now consider the case where the RWA begins to breakdown, and the counter-rotating terms must be taken into account. In this scenario, the multioscillator Hamiltonian in the non-RWA dispersive regime becomes

$$\begin{aligned} \hat{H}_{\text{Disp}}^{\text{MO}} \simeq & \sum_k \omega_k \hat{a}_k^\dagger \hat{a}_k + \frac{\omega_q}{2} \hat{\sigma}_z \\ & + \sum_k (\chi_k + \xi_k) \hat{\sigma}_z \left(\frac{1}{2} + \hat{a}_k^\dagger \hat{a}_k \right) \\ & + \sum_{j>k} \frac{(\tilde{\chi}_{j,k} + \tilde{\xi}_{j,k})}{2} \hat{\sigma}_z (\hat{a}_j^\dagger + \hat{a}_j) (\hat{a}_k^\dagger + \hat{a}_k). \end{aligned} \quad (17)$$

In this regime, the qubit-conditional interactions include both a beamsplitter and two-mode squeezing interaction (non-excitation preserving). The presence of both terms allows for different continuous variable gates such as a qubit-controlled SUM gate or a qubit-controlled-control-Z gate [43, 49].

III. SINGLE QUBIT-OSCILLATOR MULTIPHOTON INTERACTION DISPERSIVE REGIME

In the previous section, we highlighted the essence of the RWA and non-RWA dispersive regimes when linear interactions are at play between a single qubit and an oscillator, multiple qubits and an oscillator, and finally, multiple oscillators and a qubit. In this section, we begin by introducing the single qubit-oscillator multiphoton generalizations of interest: the n -Rabi (n R) model and its sister model, the n -photon Jaynes-Cummings (n JC) model. We also discuss some of the mathematical complications arising for the n R and n JC Hamiltonians in the case of $n > 2$ as well as their remedies. Then, we proceed to develop the multiphoton generalization of the SW transformations presented in the previous section.

The Hamiltonian of the n R model reads

$$\hat{H}_{n\text{-R}} = \omega_o \hat{a}^\dagger \hat{a} + \frac{\omega_q}{2} \hat{\sigma}_z + g_n \hat{\sigma}_x (\hat{a}^{\dagger n} + \hat{a}^n), \quad (18)$$

where g_n is the n -photon coupling strength. It is worth noting that this model is highly relevant for quantum information and quantum optics as its interaction is in the form of a qubit-conditional (generalized) squeezing generator, $g_n \hat{\sigma}_x (\hat{a}^{\dagger n} + \hat{a}^n)$, which is of importance for synthesizing gates and for interferometry. There is a similar model and its interaction Hamiltonian is $g_n \hat{\sigma}_x (\hat{a}^\dagger + \hat{a})^n$, which we refer to as the full n R model. The full n R model naturally arises when studying physical implementations of non-dipolar qubit-oscillator interactions [24]. The n R and n JC interaction terms are more commonly studied

than the full n R model due to their relevance for quantum information applications. It is worth noting that for weak coupling strengths, all three models are equivalent descriptions¹. Apart from some commentary in the introductory part of this section, we do not concern ourselves with the full n R model in this paper.

When the qubit and oscillator are near n -photon resonance, $\omega_q \simeq n\omega_o$, and the coupling strength is small compared to the qubit and oscillator frequencies, the effects of the counter-rotating terms, $\hat{\sigma}_+ \hat{a}^{\dagger n}$ and $\hat{\sigma}_- \hat{a}^n$, become negligible. Explicitly, when the coupling strength and qubit and oscillator frequencies satisfy

$$|\Delta_n| \ll \Sigma_n \text{ and } g_n \ll \omega_o, \quad (19)$$

where $\Delta_n = \omega_q - n\omega_o$ and $\Sigma_n = \omega_q + n\omega_o$, the n R Hamiltonian can be simplified to the n JC Hamiltonian,

$$\hat{H}_{n\text{-R}} \simeq \hat{H}_{n\text{-JC}} = \omega_o \hat{a}^\dagger \hat{a} + \frac{\omega_q}{2} \hat{\sigma}_z + g_n (\hat{\sigma}_+ \hat{a}^n + \hat{\sigma}_- \hat{a}^{\dagger n}). \quad (20)$$

As in the linear interaction ($n = 1$) case, the n JC model is exactly solvable and its spectra can be analytically computed [7]. The n JC model predicts singlets for the states $|g, k\rangle$, where $k < n$. The singlets are followed by doublets that separate and eventually cross [10–12].

A key phenomenon occurring in the n R model for $n = 2$ is that of spectral collapse, where the discretely indexed states and spectra collapse to a continuum. This collapse happens at a critical coupling ratio $r_c = g_2/\omega_o = 1/2$. There have been some explanations such as the qubit inducing an inversion of the oscillator's potential which admits no bound states [50]. It is worth noting that the full n R model for $n = 2$ exhibits the same type of spectral collapse at $r_c \simeq 1/4$ [24]. Interestingly, in the two-photon JC model, a spectral ‘bunching’ of one energy level out of each doublet (those with a negative sign; see Eq. (22)) where all these energy levels cross each other at $g_2/\omega_o \simeq 1$ and deviate again. While this is an interesting mathematical feature, it is important to note that this spectral bunching in the two-photon JC model occurs well beyond its regime of validity (see Eq. (19)).

The n R model for $n > 2$ suffers from spectral instabilities due to the unboundedness of the Hamiltonian from below which leads to states with infinite negative energies at any nonzero coupling ($g_n > 0$). This means that calculations even for low coupling strengths will be plagued by the infinite negative energies affecting the Hamiltonian spectrum. Other studies have shown that the n R model for $n > 2$ is, strictly speaking, not self adjoint and, thus, they concluded it is unphysical [51]. It is important to note that the n JC Hamiltonian while exactly solvable also suffers from negative infinite energies. This

¹ Explicitly, the n JC model serves as an excellent approximation for the full n R and n R models in the weak coupling regime.

becomes obvious when expressing the n JC Hamiltonian in the following form:

$$\hat{H}_{n\text{JC}} = \sum_{k=0}^{n-1} (E_{g,k} |g, k\rangle \langle g, k|) + \bigoplus_{l=0}^{\infty} \left(\begin{array}{cc} \omega_q/2 + l\omega_o & g_n \sqrt{(l+1)\dots(l+n)} \\ g_n \sqrt{(l+1)\dots(l+n)} & -\omega_q/2 + (l+n)\omega_o \end{array} \right), \quad (21)$$

where the 2×2 matrices act on the subspaces spanned by $\{|e, l\rangle, |g, l+n\rangle\}$ for nonnegative integers l . This form explicitly shows the aforementioned singlets and doublets which are represented by the first and second terms, respectively. To show the negative infinite energies, we can simply obtain the doublet energies by diagonalize the 2×2 matrix in each fixed l subspace;

$$E_{\pm, l}^{(n)} = \left(l + \frac{n}{2}\right) \omega_o \pm \sqrt{g_n^2 (l+n)! / l! + \Delta_n^2}. \quad (22)$$

For very large l , the second term (under the square root) scales as $l^{n/2}$ while the first term which is strictly positive, scales as l . This means that there are infinitely many states with infinite negative energies for all $n > 2$. Even though the n JC Hamiltonian is exactly solvable, it is also problematic because it is unbounded from below. However, when studying the n R or n JC Hamiltonian, one must keep in mind that, in practice, these models never arise as the sole terms in a realistic system Hamiltonian. Rather, they are arrived at as an effective description in a weak-coupling and low-energy regime. These effective descriptions typically neglect other terms that bound these spectral instabilities such as unbounded states (see, for example, the derivations of effective multiphoton Hamiltonians in Refs [22] and [52], where spurious terms that make the total system Hamiltonian bounded are neglected to obtain similar effective descriptions).

In this paper, we are interested in the study of the dispersive regime of multiphoton qubit-oscillator interactions by means of SW second-order perturbation theory. As with typical use cases of SW-type perturbation theory, we seek to obtain effective low-energy descriptions decoupled from the high-energy subspaces of the system [53]. Thus, for completeness, we can remedy the aforementioned spectral instabilities caused by the unboundedness of the n R and n JC Hamiltonians by considering them as an approximation of more realistic Hamiltonians that contain additional bounding terms that stabilize the high-photon-number part of the Hilbert space. Such terms avoid the issues of infinite negative energies by bounding the Hamiltonians from below. These terms will have a very small coupling strength and will only affect the high-photon-number states of the system and will not alter the low-energy effective descriptions we seek. Thus, we add a bounding term to the n R Hamiltonian

such that it reads

$$\hat{H}_{n\text{-R}} = \omega_o \hat{a}^\dagger \hat{a} + \frac{\omega_q}{2} \hat{\sigma}_z + g_n \hat{\sigma}_x (\hat{a}^{\dagger n} + \hat{a}^n) + \eta g_n \hat{a}^{\dagger m_n} \hat{a}^{m_n}, \quad (23)$$

where $m_n = \lfloor n/2 \rfloor + 1$ with η being a positive real number that determines strength of the perturbation and $\lfloor x \rfloor$ denoting the floor function; we only consider cases that obey $\eta \ll 1$ such that the low-energy subspaces are barely affected by the term $\hat{a}^{\dagger m_n} \hat{a}^{m_n}$. With this perturbation, we ensure that the Hamiltonian is bounded from below. We can now study the dispersive regime of the n R (and n JC) Hamiltonian for $n > 2$ while being assured that the spectral instabilities of the high-photon-number subspaces do not affect the low-energy subspaces since, in fact, for low-energy regimes, the bounding term can be ignored.

We now proceed to develop the multiphoton generalization of the SW transformations presented in Sec. II and apply it to the n JC and n R model. We aim to use second-order SW perturbation theory to better understand the system spectra in the multiphoton dispersive regime.

A. RWA dispersive regime

We define the multiphoton RWA dispersive regime's hierarchy of energy scales as that of Eq. (19) along with

$$g_n \ll |\Delta_n|. \quad (24)$$

This allows us to define a generalized multiphoton SW transformation along with a dimensionless perturbation parameter:

$$\hat{U}_{\text{Disp,RWA}}^{(n)} := \exp\left(\lambda_n \hat{X}_{-n}\right), \quad (25)$$

where

$$\hat{X}_{\pm n} = \hat{\sigma}_- \hat{a}^{\dagger n} \pm \hat{\sigma}_+ \hat{a}^n, \quad (26)$$

and $\lambda_n = g_n / \Delta_n$. The n JC interaction term can be expressed as $g_n \hat{X}_{+n}$. Due to the parameter regime we are working in, it follows that $\lambda_n \ll 1$. We now transform the n JC Hamiltonian and expand to second order in λ_n such that the RWA dispersive Hamiltonian reads

$$\begin{aligned} \hat{H}_{\text{Disp,RWA}}^{(n)} &= \hat{U}_{\text{Disp,RWA}}^{(n)\dagger} \hat{H}_{n\text{-JC}} \hat{U}_{\text{Disp,RWA}}^{(n)} \\ &= \hat{H}_{n\text{-JC}} + \lambda_n [\hat{H}_{n\text{-JC}}, \hat{X}_{-n}] \\ &\quad + \frac{\lambda_n^2}{2} [[\hat{H}_{n\text{-JC}}, \hat{X}_{-n}], \hat{X}_{-n}] + \dots \\ &\simeq \omega_o \hat{a}^\dagger \hat{a} + \frac{\omega_q}{2} \hat{\sigma}_z + \frac{\chi_n}{2} \sum_{k=0}^n C_{n,k}^+ \hat{\sigma}_z (\hat{a}^\dagger \hat{a})^k \\ &\quad + \frac{\chi_n}{2} \sum_{k=1}^{n-1} C_{n,k}^- (\hat{a}^\dagger \hat{a})^k, \end{aligned} \quad (27)$$

TABLE I. Table of combinatorial commutator coefficients $C_{n,k}^{\pm}$ for dispersive n -photon interactions up to $n = 4$.

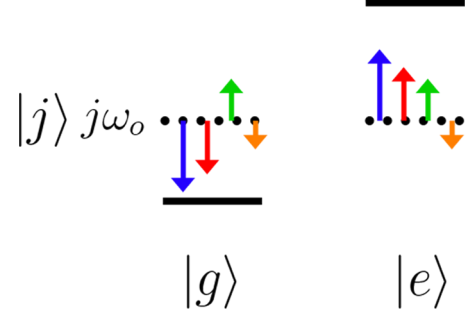
$n \setminus k$	$C_{n,k}^+$				$C_{n,k}^-$					
	0	1	2	3	4	0	1	2	3	4
1	1	2	-	-	-	1	0	-	-	-
2	2	2	2	-	-	2	4	0	-	-
3	6	13	3	2	-	6	9	9	0	-
4	24	44	46	4	2	24	56	24	16	0

where

$$C_{n,k}^{\pm} = (-1)^{n+k} s_1(n+1, k+1) \pm s_1(n, k). \quad (28)$$

Here, $s_1(n, k)$ is the Stirling number of the first kind which denotes the number of permutations of n elements which contain k permutation cycles, and $\chi_n = g_n^2/\Delta_n$ is the n -photon dispersive shift. The coefficients $C_{n,k}^{\pm}$ arise due to the combinatorics of the commutator expansion, and they have a concrete interpretation; $C_{n,k}^+$ are the commutator coefficients arising due to the qubit-state-dependent ($\hat{\sigma}_z$) part of the commutator, and $C_{n,k}^-$ arise due to the qubit-state-independent terms. Explicitly, the commutator $[\hat{X}_{+n}, \hat{X}_{-n}]$ contains $[\hat{a}^n, \hat{a}^{\dagger n}]$ which requires multiple reductions of one side of the entries to be able to evaluate it using, e.g., $[\hat{a}, f(\hat{a}^\dagger, \hat{a})] = \partial f(\hat{a}^\dagger, \hat{a})/\partial \hat{a}^\dagger$. The full derivation and simplification of the commutator into a diagonal form is found in App. A.

The Hamiltonian contains two polynomials in the photon number operator, $\chi_n \sum_{k=0}^n C_{n,k}^+ \hat{\sigma}_z (\hat{a}^\dagger \hat{a})^k$ and $\chi_n \sum_{k=0}^{n-1} C_{n,k}^- (\hat{a}^\dagger \hat{a})^k$, with the qubit-state-dependent polynomial truncating at order n and the other truncating at order $n-1$. The qubit-state-independent polynomial truncating at order $n-1$ has to do with the coefficients $C_{n,k}^-$; they are zero when $n=k$ for all n . Due to this fact, the qubit-state-dependent series causes a larger shift between energy levels. The qubit-state dependence is reflected in the sign of the shift; the shift is negative when the qubit is in $|g\rangle$, and it is positive when the qubit is in $|e\rangle$. Interestingly, for interaction orders greater than $n=2$, the qubit-oscillator interaction induces a dispersive anharmonicity in the oscillator. This usually occurs for the dispersive linear interaction ($n=1$) when accounting for expansion terms beyond second order, and due to their higher-order nature, the strength of such terms is usually very small [54]. For a given order n , the qubit-state-dependent n th order shift, as well as the lower-order dispersive shifts ($n-1, n-2, \dots$), are all present in the Hamiltonian. Interestingly, the lower-order shifts are always larger than the n th order shift as seen in the table of $C_{n,k}^+$ values; $C_{n,n}^+ = 2$ for all n . The resulting higher-order self-Kerr terms induce multiphoton blockades in the presence of a drive on the oscillator [55]. Additionally, when the oscillator is initialized in a coherent state, these higher-order self-Kerr terms can be used to make multi-component cat states [56].



	RWA	non-RWA
qubit-state independent	$\chi_n \sum_{k=1}^{n-1} C_{n,k}^- j^k$	$\xi_n \sum_{k=1}^{n-1} C_{n,k}^- j^k$
qubit-state dependent	$\chi_n \sum_{k=1}^n C_{n,k}^+ j^k$	$\xi_n \sum_{k=1}^n C_{n,k}^+ j^k$

FIG. 1. Energy-level dispersive shifts for the j th Fock state. The qubit-state-independent shifts in the RWA (green) and non-RWA (orange) cases are always weaker than the qubit-state-dependent RWA (blue) and non-RWA (red) shifts. This is due to the fact that the former's polynomial is of degree $n-1$, while the polynomial of the latter is of degree n . Additionally, both RWA shifts are larger than the non-RWA shifts since $\chi_n > \xi_n$.

B. Non-RWA dispersive regime

When the first inequality of Eq. (19) no longer holds, it is possible to extend the usefulness of the SW transformation by adding another generator which accounts for the counter-rotating terms. Thus, as performed in Sec. II, we resort to an additional generator in the SW transformation and apply it to the n R model which includes the counter-rotating terms. We now define the multiphoton non-RWA dispersive regime in a similar fashion to the case of the linear interaction [29]. The non-RWA regime obeys

$$g_n \ll |\Delta_n|, \quad (29)$$

where $|\Delta_n| \ll \Sigma_n$ is no longer necessarily true. Thus, this paves the way for the generalized non-RWA SW transformation:

$$\hat{U}_{\text{Disp}}^{(n)} := \exp\left(\lambda_n \hat{X}_{-n} + \bar{\lambda}_n \hat{Y}_{-n}\right), \quad (30)$$

where

$$\hat{Y}_{\pm n} = \hat{\sigma}_- \hat{a}^n \pm \hat{\sigma}_+ \hat{a}^{\dagger n} \quad (31)$$

and $\bar{\lambda}_n = g_n/\Sigma_n$. Here, $\hat{X}_{\pm n}$ and $\hat{Y}_{\pm n}$ do not commute, just as in the linear case. Equation (29) ensures that

$\bar{\lambda}_n, \lambda_n \ll 1$ and allows for the perturbative expansion using $\hat{U}_{\text{Disp}}^{(n)}$ to second order in $\bar{\lambda}_n$ and λ_n . Then, the non-RWA dispersive Hamiltonian reads

$$\begin{aligned} \hat{H}_{\text{Disp}}^{(n)} &= \hat{U}_{\text{Disp}}^{(n)\dagger} \hat{H}_{n\text{-R}} \hat{U}_{\text{Disp}}^{(n)} \\ &= \hat{H}_{n\text{-R}} + [\hat{H}_{n\text{-R}}, \lambda_n \hat{X}_{-n} + \bar{\lambda}_n \hat{Y}_{-n}] \\ &\quad + \frac{1}{2} [\hat{H}_{n\text{-R}}, \lambda_n \hat{X}_{-n} + \bar{\lambda}_n \hat{Y}_{-n}, \\ &\quad \lambda_n \hat{X}_{-n} + \bar{\lambda}_n \hat{Y}_{-n}] + \dots \\ &\simeq \omega_o \hat{a}^\dagger \hat{a} + \frac{\omega_q}{2} \hat{\sigma}_z + \frac{(\chi_n + \xi_n)}{2} \sum_{k=0}^n C_{n,k}^+ \hat{\sigma}_z (\hat{a}^\dagger \hat{a})^k \\ &\quad + \frac{(\chi_n - \xi_n)}{2} \sum_{k=1}^{n-1} C_{n,k}^- (\hat{a}^\dagger \hat{a})^k \\ &\quad + \frac{(\chi_n + \xi_n)}{2} \hat{\sigma}_z (\hat{a}^{\dagger 2n} + \hat{a}^{2n}), \end{aligned} \quad (32)$$

where $\xi_n = g_n^2/\Sigma_n$ is the n -photon Bloch-Siegert shift coefficient. The non-RWA regime transformation yields an additional shift, ξ_n , dependent on the counter-rotating terms which in turn oscillate with $\omega_q + n\omega_o$. The commutators $[\hat{X}_{+n}, \hat{Y}_{-n}]$, $[\hat{Y}_{+n}, \hat{X}_{-n}]$, and $[\hat{Y}_{-n}, \hat{Y}_{+n}]$ give rise to the same combinatorial coefficients as $[\hat{X}_{+n}, \hat{X}_{-n}]$ and are also discussed in App. A. The non-RWA regime Hamiltonian exhibits a generalized $2n$ -photon squeezing term, $\hat{\sigma}_z (\hat{a}^{\dagger 2n} + \hat{a}^{2n})$. This is consistent with the one-photon dispersive calculations presented in Sec II. Unlike in the RWA regime, here, the qubit-state-independent oscillator anharmonicity is negative and pushes the energy levels down.

The different shifts arising in the RWA and non-RWA dispersive regime are summarized in Fig. 1. Generally, the RWA effects are stronger than the non-RWA effects since $\chi_n > \xi_n$.

Note that the non-RWA Hamiltonian is not diagonal in the bare basis. An easy remedy is to add the generator of the qubit-conditional $2n$ -photon squeezing term [30],

$$\hat{U}_{\text{Disp}}^{(n)} := \exp\left(\lambda_n \hat{X}_{-n} + \bar{\lambda}_n \hat{Y}_{-n} + \zeta_n \hat{Z}_n\right) \quad (33)$$

where $\zeta_n = g_n \bar{\lambda}_n / 2n\omega_o$ and

$$\hat{Z}_n = \hat{\sigma}_z (\hat{a}^{2n} - \hat{a}^{\dagger 2n}). \quad (34)$$

With this transformation, the generalized $2n$ -photon squeezing term vanishes, and the non-RWA Hamiltonian becomes diagonal to second order in $\bar{\lambda}_n$ and λ_n . Then, we may analytically find the spectra of the system as

$$\begin{aligned} E_j^{e/g}(n) &= \langle e/g | \langle j | \hat{H}_{\text{Disp}}^{(n)} | e/g \rangle | j \rangle \\ &= \omega_o j + \frac{(\chi_n - \xi_n)}{2} \sum_{k=1}^{n-1} C_{n,k}^- j^k \\ &\quad \pm \frac{(\chi_n + \xi_n)}{2} \sum_{k=1}^n C_{n,k}^+ j^k \pm \frac{\omega_q}{2}, \end{aligned} \quad (35)$$

where $\hat{H}_{\text{Disp}}^{(n)}$ is the non-RWA Hamiltonian without the $2n$ -photon squeezing term. From this last equation, we can set $\xi_n = 0$ to obtain the RWA spectrum. Generally, if we transform to the usual interaction picture via $\exp(-i\omega_q t \hat{\sigma}_z / 2 - i\omega_o t \hat{a}^\dagger \hat{a})$, when the energy scales follows Eq. (19), ξ_n will be negligibly small and we can drop the fast-oscillating $2n$ -photon squeezing terms, $\hat{a}^{\dagger 2n}$ and \hat{a}^{2n} , which allows us to recover the RWA results.

C. Comparison with numerical results

We now compare the analytically derived results of the RWA and non-RWA spectra with the numerically-obtained spectra of the n R model [Eq. (23) with $\eta = 0.01$]. We prelude the discussion with a reminder of the looming spectral instabilities for higher orders of n . The spectral instabilities of the n R model for $n > 2$ restrict the low-energy regime in a smaller set of parameters than $n = 2$. Thus, the low-energy stable regime shrinks for higher-order interactions. This means that, in general, the regime of validity for the perturbation theory becomes smaller for larger n . Additionally, the dispersive regime where the qubit-oscillator system can be approximately described in its bare basis comprises a smaller range of parameters for higher orders of n . Another issue to keep in mind is the fact that the usual non-RWA effects become non-negligible for larger g_n/ω_o — at least in the usual linear case. This suggests the need for a spectral classification of the n R model that is distinct from the spectral classification of the typical linear Rabi model as in Refs. [57, 58].

In Fig. 2, we compare the analytical results from second-order SW perturbation theory with numerical diagonalization of the n R Hamiltonian². We start by noting general trends. The description provided by perturbation theory significantly improves when λ_n (and $\bar{\lambda}_n$) gets smaller, as expected. This is seen in the improvement of overlap between the numerical and analytical spectra between Fig. 2(a) and (b) for $n = 2$, and (c) and (d) for $n = 3$, where the ranges of λ_n (and $\bar{\lambda}_n$) become smaller for higher $|\Delta_n|$. The deviation from the analytic description occurs in a similar fashion to the deviation

² In the case of $n = 2$, the numerically-obtained spectra match the quasi-analytic solutions of Refs. [16, 17]

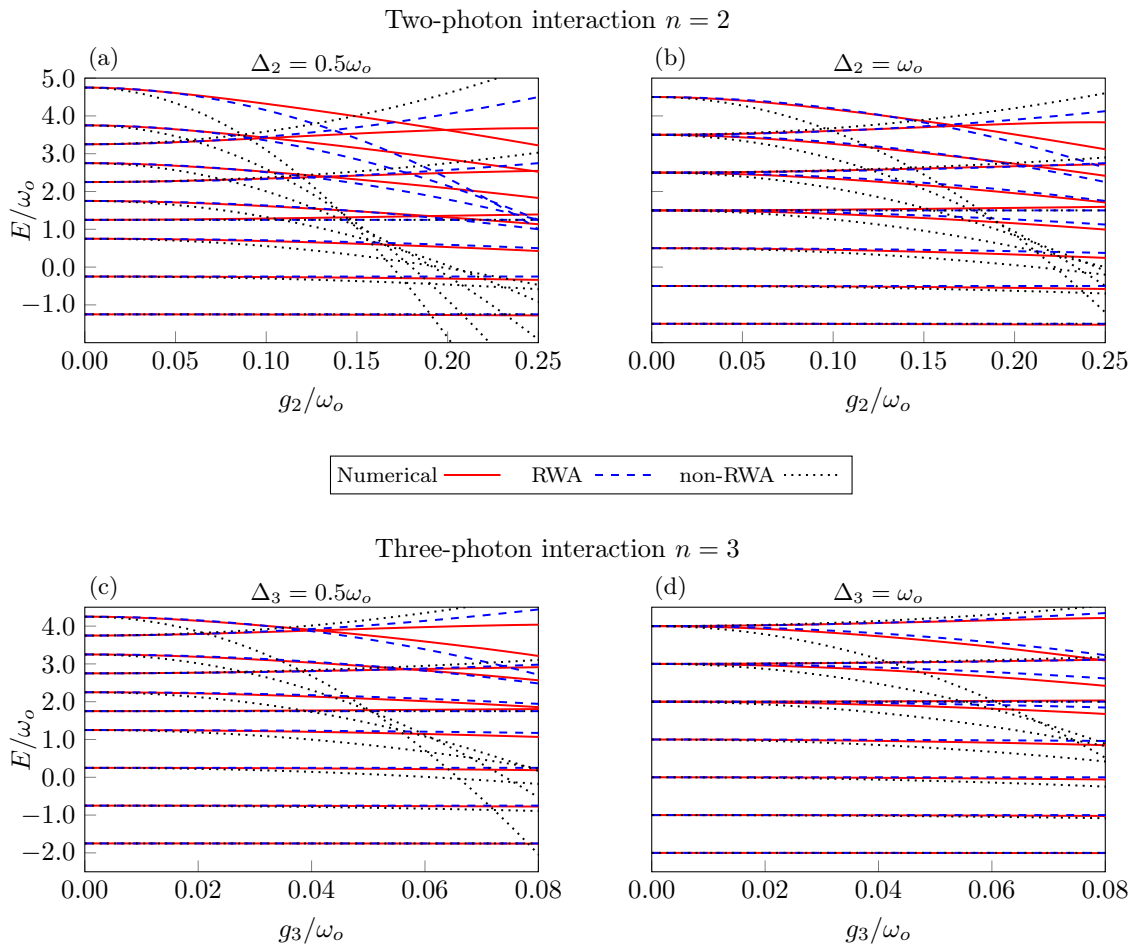


FIG. 2. Multiphoton qubit-oscillator interaction spectra in the dispersive regime. The analytic spectra from the RWA and non-RWA perturbative expansions are compared with the numerically-obtained spectra of Eq. (23) with $\eta = 0.01$. For each plot, Δ_n is fixed, and, as such, the x -axis (g_n) can be thought of as tuning the perturbation parameters λ_n and $\bar{\lambda}_n$. The analytic results, in general, deviate at smaller coupling strengths, or, equivalently, perturbation parameters, for higher-order interactions (see (a/b) compared to (c/d)). The non-RWA spectra deviates at smaller coupling strengths than its RWA counterpart. Additionally, the higher-energy levels RWA and non-RWA analytic spectra deviate at smaller coupling strengths.

of the general nR spectra from the nJC spectra in two ways. The first trend is one within a fixed interaction order; the higher energy levels deviate at smaller ratios of g_n/ω_o . The second trend is that the higher-order interactions deviate at smaller ratios of g_n/ω — this can be immediately attributed to the smaller dispersive regime for higher-order interactions as discussed earlier. Figures 2(c) and (d) show the dispersive regime for $n = 3$, and we observe the two trends noted above; locally for a fixed interaction order, the higher energy levels deviate at smaller coupling strengths, and globally when comparing (a) and (b) to (c) and (d), the higher-order interactions comprise a smaller range of parameters in the dispersive regime.

A surprising occurrence is the deviation of the non-RWA analytical spectra from the numerical calculations in many instances at smaller coupling strengths than the RWA spectra. In other words, the non-RWA results are a

worse approximation than the RWA results. This can be seen in Fig. 2. This suggests that the role of the counter-rotating terms in nR model is not well-represented in the non-RWA SW transformation. Thus, a simple extension of the generators in the generalized multiphoton SW transformation is not enough to extend the validity of the perturbative expansion spectra. This is very different from the linear interaction where the non-RWA generators extend the validity of the perturbative expansion and analytic spectra to regimes of larger coupling strengths [29, 30].

D. Experimental signature of dispersive multiphoton qubit-oscillator interactions

In the previous sections, we presented the analytical perturbation theory results and established a regime of

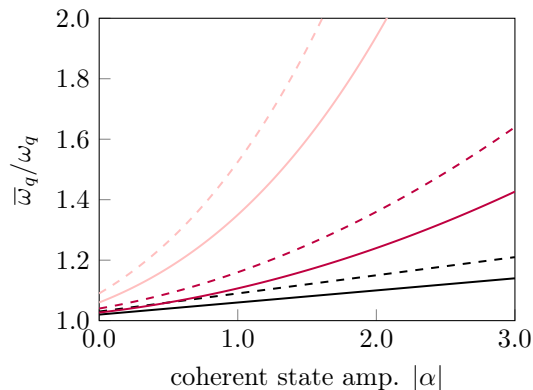


FIG. 3. Effective qubit frequency due differing interaction orders as a function of oscillator coherent state amplitude. The ratio of effective qubit frequency to bare qubit frequency is plotted as a function of the amplitude of the coherent state populating the oscillator. The black, purple and pink lines correspond to $n = 1$, $n = 2$ and $n = 3$ dispersive interactions, respectively; solid lines represent $g_n = 0.02\omega_o$ and dashed lines represent $g_n = 0.03\omega_o$.

validity in comparison with numerical results. Here, we seek to highlight a signature of the multiphoton dispersive interactions to test the differing interaction orders. Furthermore, we provide estimates for the dispersive regime couplings and shifts based on realistic circuit QED implementation proposals [22, 24].

As the RWA perturbation theory proved to be more effective than its non-RWA counterpart, we rely on the Hamiltonian of Eq. (27). We consider the effective (dressed) qubit frequency as a function of the oscillator population and its powers,

$$\bar{\omega}_q^{(n)} = \omega_q + \chi_n \sum_{k=0}^n C_{n,k}^+ \langle (\hat{a}^\dagger \hat{a})^k \rangle, \quad (36)$$

where the oscillator occupation dresses the qubit frequency in a manner dependent on the interaction order. For an experimentally-motivated illustration, let us consider the oscillator to be occupied by a coherent state $|\alpha\rangle$, where $\langle \hat{a}^\dagger \hat{a} \rangle = |\alpha|^2$. Here, we can imagine the oscillator being populated by some external linear drive $\propto (\hat{a}^\dagger \pm \hat{a})$. Using the identity $(\hat{a}^\dagger \hat{a})^k = \sum_{l=0}^k s_2(k, l) \hat{a}^{\dagger l} \hat{a}^l$ [59], we can now easily evaluate $\langle \alpha | (\hat{a}^\dagger \hat{a})^k | \alpha \rangle = \sum_{l=0}^k s_2(k, l) |\alpha|^l$. We may now observe the growth in the effective qubit frequency as a function of the amplitude of the coherent state, $|\alpha|$, populating the oscillator. Figure 3 shows the trends in effective qubit frequency for different interaction orders, n , for two different g_n values at each order. Notably, the growth of the shift is a polynomial of degree n . The difference in growth behaviour of the effective qubit shifts as a function of coherent state amplitude serves as a potential experimental signature for distinguishing $n = 1$, $n = 2$ and $n = 3$ (and beyond) dispersive interactions.

In the case of $n = 2$, for a superconducting circuit

implementation, we can provide realistic estimates of the qubit-oscillator system parameters in the dispersive regime and the corresponding shifted effective qubit frequency. For a qubit frequency $\omega_q = 2\pi \times 13.5$ GHz and oscillator frequency $\omega_o = 2\pi \times 4.50$ GHz, i.e. $\Delta_2 = \omega_o$, there are circuit design proposals with g_2 anywhere from 25 MHz [22] up to $g_2 \sim 1$ GHz [25]. For a simple estimate in the dispersive regime, we can choose $g_2 = 90$ MHz ($= 0.02\omega_o$) with $\chi_2 = 3.6$ MHz. We can extract the qubit shift, $\delta\omega_q = \bar{\omega}_q - \omega_q$, as a function oscillator coherent state population using the solid purple line in Fig. 3. As an example, when the oscillator is populated with a coherent state with amplitude $|\alpha| = 1$, the qubit shift will be $\delta\omega_q \simeq 1.45$ GHz. This shift is measurable and can be used to verify our predictions of the multiphoton dispersive regime.

IV. MULTIPLE QUBITS COUPLED TO A SINGLE OSCILLATOR

With the established technique from the single qubit-oscillator multiphoton dispersive regime, we now move on to the multipartite scenario where N qubits are coupled to a shared oscillator through an n -photon interaction.

We begin with the n -photon Dicke (nD) Hamiltonian (generalizing from Sec. II) whose Hamiltonian reads

$$\hat{H}_{n-D}^N = \omega_o \hat{a}^\dagger \hat{a} + \sum_{l=1}^N \frac{\omega_q^{(l)}}{2} \hat{\sigma}_z^{(l)} + \sum_{l=1}^N g_n^{(l)} (\hat{\sigma}_+^{(l)} + \hat{\sigma}_-^{(l)}) (\hat{a}^n + \hat{a}^{\dagger n}), \quad (37)$$

where we recall that the superscript (l) denotes the l th qubit. Of course, just as in the linear case, when each of the qubits is individually in the n JC energy-scale regime, we can simplify the nD Hamiltonian by applying an RWA, as done in the single qubit-oscillator case. This leads us to the n -photon Tavis-Cummings Hamiltonian (nTC),

$$\hat{H}_{n-TC}^N = \omega_o \hat{a}^\dagger \hat{a} + \sum_{l=1}^N \frac{\omega_q^{(l)}}{2} \hat{\sigma}_z^{(l)} + \sum_{l=1}^N g_n^{(l)} (\hat{\sigma}_+^{(l)} \hat{a}^n + \hat{\sigma}_-^{(l)} \hat{a}^{\dagger n}). \quad (38)$$

The nTC model is exactly solvable, and just like the nJC model, the nTC Hamiltonian predicts $2N(n-1)$ singlets followed by doublets. Here, there are N -times the singlets and doublets of the single-qubit model due to the additional qubits.

The spectral collapse for $n = 2$ persists in the multiqubit case. The presence of multiple qubits changes the critical coupling at which the collapse occurs. It was shown for the case of $n = 2$ that the collapse occurs at a

smaller collective critical collapse coupling [24]. Explicitly, for a fixed oscillator frequency, if we take a single qubit-oscillator system where the critical collapse coupling is $g_{2,c}$, the individual qubit couplings at which the multipartite system's spectral collapse occurs are all less than the single qubit case, $g_2^{(1)}, \dots, g_2^{(N)} < g_{2,c}$; the shifted multipartite (N qubit) critical collapse coupling $\tilde{g}_{2,c}^N$ is less than $g_{2,c}$ due to coupling enhancement in Dicke-type models. When all individual couplings are the same, the enhancement scales as \sqrt{N} . For varying individual coupling strengths, there is no simple scaling factor describing the enhancement of the individual coupling strengths. However, some approximate relations can be derived, for example using a mean-field treatment of the interactions between the different subsystems [60]. Additionally, the discussion on the spectral instabilities for $n > 2$ follows from the single qubit-oscillator case and applies just as well. Figure 4 shows the n D Hamiltonian spectra (in red) for a two-qubit system ($N = 2$). Here, we detune one qubit above the oscillator frequency and the other below it where both possess an n -photon detuning of $|\Delta_n^{(1)}| = |\Delta_n^{(2)}| = \omega_o$. For a single plot in Fig. 4, the qubits and oscillator frequencies are fixed as well as one of the qubits' coupling strengths. Then, we can see the effect of changing the other qubit's coupling strength on the spectra in general and the spectral collapse in particular.

A. RWA dispersive regime

We may now generalize the multiphoton dispersive regime and its SW transformation of the single qubit-oscillator case to the case of multiple qubits. We start with the RWA regime where the qubits all obey $g_n^{(j)} \ll |\Delta_n^{(j)}|$. Next, we straightforwardly generalize the generators to be a sum over the qubit indices, and the parameters are now also labelled with the same indices. Then, the multiqubit SW transformation reads as

$$\hat{U}_{\text{Disp,RWA}}^{(n)} := \exp\left(\sum_j \lambda_n^{(j)} \hat{X}_{-n}^{(j)}\right). \quad (39)$$

Similarly, we transform the Hamiltonian and expand to first order in all the perturbation parameters to obtain

$$\begin{aligned} \hat{H}_{\text{Disp,RWA}}^{N,(n)} &= \hat{U}_{\text{Disp,RWA}}^{(n)\dagger} \hat{H}_{n\text{-TC}}^N \hat{U}_{\text{Disp,RWA}}^{(n)} \\ &= \hat{H}_{n\text{-TC}}^N + \sum_l \lambda_l [\hat{H}_{n\text{-TC}}^N, \hat{X}_{-n}^{(l)}] \\ &\quad + \sum_{l,m} \frac{\lambda_l \lambda_m}{2} [[\hat{H}_{n\text{-TC}}^N, \hat{X}_{-n}^{(l)}], \hat{X}_{-n}^{(m)}] + \dots \\ &\simeq \sum_l \hat{H}_{\text{Disp,RWA}}^{(l),(n)} \\ &\quad + \sum_{l>m} \sum_{k=0}^{n-1} \left[\tilde{\chi}_n^{(l,m)} C_{n,k}^- (\hat{\sigma}_+^{(l)} \hat{\sigma}_-^{(m)} + \hat{\sigma}_-^{(l)} \hat{\sigma}_+^{(m)}) (\hat{a}^\dagger \hat{a})^k \right] \end{aligned} \quad (40)$$

where

$$\tilde{\chi}_n^{(l,m)} = g_n^{(l)} g_n^{(m)} \left(\frac{1}{\Delta_n^{(l)}} + \frac{1}{\Delta_n^{(m)}} \right),$$

and $\hat{H}_{\text{Disp,RWA}}^{(l),(n)}$ is the l^{th} qubit RWA dispersive Hamiltonian of Eq. (27). In this case, a photon-number dependent oscillator-mediated qubit-qubit interaction emerges. The qubit-qubit interaction between the l th and m th qubits vanishes if $\Delta_n^{(l)} = -\Delta_n^{(m)}$ since in this case $\tilde{\chi}_n^{(j,k)} = 0$. Similarly to the linear interaction, the RWA regime gives rise to an anisotropic XY excitation-preserving qubit-qubit interaction of the form $\hat{\sigma}_+^{(l)} \hat{\sigma}_-^{(m)} + \text{H.c.}$.

B. Non-RWA dispersive regime

We now proceed to generalize the single qubit-oscillator non-RWA dispersive regime to the case of multiple qubits. Here, the energy scale in effect obeys $g_n^{(j)} \ll |\Delta_n^{(j)}|, \Sigma_n^{(j)}$ for each qubit. To this extent, we use the non-RWA generalized SW transformation with a sum of generators over the qubit indices such that the unitary reads

$$\hat{U}_{\text{Disp}}^{(n)} := \exp\left(\sum_j \lambda_n^{(j)} \hat{X}_{-n}^{(j)} + \sum_j \bar{\lambda}_n^{(j)} \hat{Y}_{-n}^{(j)}\right). \quad (41)$$

Then, the multiqubit non-RWA dispersive Hamiltonian, up to first order in all perturbation parameters, is ex-

panded as

$$\begin{aligned}
\hat{H}_{\text{Disp}}^{N,(n)} &= \hat{U}_{\text{Disp}}^{(n)\dagger} \hat{H}_{n-D}^N \hat{U}_{\text{Disp}}^{(n)} \\
&= \hat{H}_{n-D}^N + \sum_l [\hat{H}_{n-D}^N, \lambda_l \hat{X}_{-n}^{(l)} + \bar{\lambda}_l \hat{Y}_{-n}^{(l)}] \\
&\quad + \sum_{l,m} \left[[\hat{H}_{n-D}^N, \lambda_l \hat{X}_{-n}^{(l)} + \bar{\lambda}_l \hat{Y}_{-n}^{(l)}], \right. \\
&\quad \quad \left. \lambda_m \hat{X}_{-n}^{(m)} + \bar{\lambda}_m \hat{Y}_{-n}^{(m)} \right] + \dots \\
&\simeq \sum_{l=1}^N \hat{H}_{\text{Disp}}^{(l),(n)} \\
&\quad + \sum_{l>m} \sum_{k=0}^{n-1} \left[(\tilde{\chi}_n^{(l,m)} - \tilde{\xi}_n^{(l,m)}) C_{n,k}^- (\hat{\sigma}_x^{(l)} \hat{\sigma}_x^{(m)}) (\hat{a}^\dagger \hat{a})^k \right]
\end{aligned} \tag{42}$$

where

$$\tilde{\xi}_n^{(l,m)} = g_n^{(l)} g_n^{(m)} \left(\frac{1}{\Sigma_n^{(l)}} + \frac{1}{\Sigma_n^{(m)}} \right),$$

and $\hat{H}_{\text{Disp}}^{(l),(n)}$ is the l^{th} qubit non-RWA dispersive Hamiltonian of Eq. (32). As expected, the non-RWA dispersive regimes gives rise to an Ising-type oscillator-mediated qubit-qubit interaction. Here, the qubit-qubit interaction is also enhanced by the photon-number coupling, but the coupling strength diminishes due to the $-\tilde{\xi}_n^{(l,m)}$ non-RWA coefficient. One can also eliminate the $2n$ -photon squeezing terms by applying the extended transformation of Eq. (33).

C. Comparison with numerical results

We now compare the perturbative expansion calculations with the numerical results. Specifically, we focus on the two-qubit nD model for $n = 2$.

It is possible to exactly diagonalize the RWA Hamiltonian of Eq. (40) by simply diagonalizing the two-qubit system. Essentially, the Hamiltonian becomes a block-diagonal matrix of 4×4 blocks. Similarly, in the non-RWA case, we can first apply the extended transformation accounting for the $2n$ -photon squeezing term presented in Eq. (33), and then diagonalize the two-qubit part of the Hamiltonian. We now compare the numerically obtained spectra to those analytically obtained from the RWA and non-RWA Hamiltonians.

The analytical spectra produced by the RWA and non-RWA expansions are contrasted with the numerical spectra of the two-qubit two-photon Dicke Hamiltonian in Fig. 4. For a single plot, we fix one qubit's coupling to the oscillator and we vary the other qubit's coupling. Here, we assume $\Delta_2^{(1)} = -\Delta_2^{(2)} = \omega_o$. It is important to note that in this case, the RWA Hamiltonian predicts the vanishing of the mediated photon-number-enhanced qubit-qubit interaction as $\tilde{\chi}_2^{(1,2)} = 0$. Meanwhile, the non-RWA

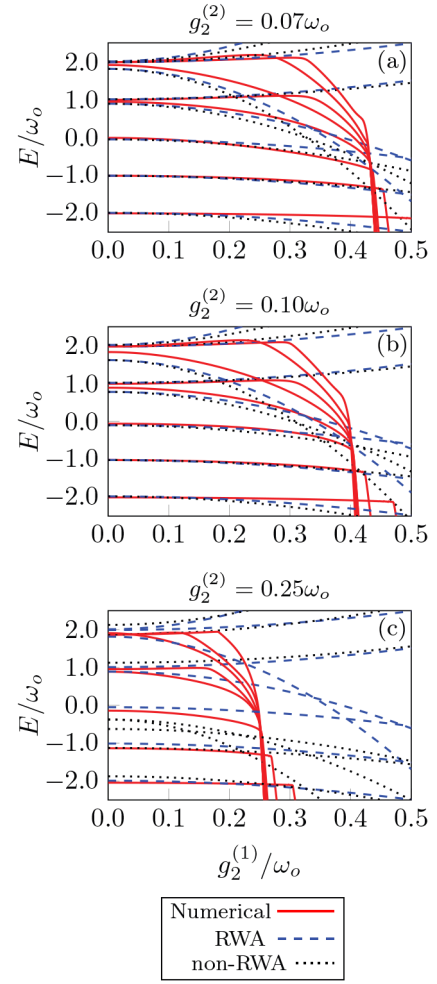


FIG. 4. Spectra of the two-qubit two-photon Dicke model contrasted with perturbative spectra. We assume $|\Delta_2^{(j)}| = \omega_o$; one qubit is detuned above the oscillator frequency and the other is detuned below. In this case, $\tilde{\chi}_2^{(1,2)} = 0$. Solid lines represent numerical results, dashed lines represent RWA analytical results, and dotted lines represent non-RWA analytical results. For each plot we fix the two qubit frequencies, oscillator frequency and one of the qubits' coupling strengths. The coupling strength of the other qubit is varied, and the spectra are plotted as a function of it. The spectral collapse shifts to smaller critical coupling ratios which occurs due to the collective qubit cooperative effects. The RWA results generally provide an accurate description in the low collective coupling regimes, but the non-RWA predictions deviate more rapidly from the numerical spectra. For higher collective coupling (sum of individual couplings), the accuracy of perturbative results becomes less accurate (see main text for detailed commentary).

Hamiltonian predicts its persistence as $\tilde{\xi}_2^{(1,2)} \neq 0$, which should significantly affect the resulting spectra. Figure 4(a) shows the regime where the fixed qubit coupling is well in its single qubit-oscillator dispersive regime, i.e. $g_2^{(2)} \ll g_{2,c}$ with $g_{2,c}$ being the single qubit-oscillator two-photon critical collapse coupling. In this regime, the collective qubit cooperative effects is relatively weak which

only slightly shifts the aforementioned collective critical collapse coupling, $\tilde{g}_{n,c}^N$ ($N = n = 2$), slightly lower than $g_{n,c}$. We find that the perturbative spectra shows very similar trends to the single qubit-oscillator case; the lower-energy states better match the numerical results, and the RWA expansion generally better approximates the system whereas the non-RWA predictions deviate at lower coupling strengths. When both qubits' couplings are in the single qubit-oscillator dispersive regime, i.e. $g_2^{(j)} \ll |\Delta_2|^{(j)}$, $|\Delta_2|^{(2)}$, $g_{2,c}$ ($j = 1, 2$), the perturbative description of the system is in excellent match with the numerics. However, when the one of the qubits is outside its individual regime of validity, the collective critical collapse coupling shifts more significantly as shown in Figs. 4(b) and (c). This also results in the deviation of the perturbative spectra and, so, they become valid in for a smaller range of parameters. The non-RWA spectra significantly deviate in the case higher-energy states in Fig. 4(b). This is because the non-RWA Hamiltonian's qubit-qubit interaction term does not vanish and with growing qubit coupling strengths and higher Fock states—hence higher energy states—becomes a significant contribution. This reaffirms the conclusion of the single qubit-oscillator results where the non-RWA extension of the SW transformation becomes a less accurate description particularly, for higher-energy states and generally, at lower coupling strengths.

D. Oscillator-mediated tunably coupled multiqubit system

The photon-number dependence of the mediated qubit-qubit interaction allows for the tuning of the effective qubit frequencies and mediated qubit-qubit coupling by carefully selecting the oscillator state. As an example, we can take two qubits interacting with an oscillator via an n -photon interaction. Since the RWA expansion results in a better approximation than the non-RWA case, we consider the RWA Hamiltonian of Eq. (40). Similarly to the calculations carried out in Sec. IIID, we consider the oscillator to be populated by a coherent state $|\alpha\rangle$. We now consider the effective two-qubit Hamiltonian. Then, the effective Hamiltonian (ignoring constant offsets) is

$$\begin{aligned} \hat{H}_{\text{Eff}} &= \langle \alpha | \hat{H}_{\text{Disp,RWA}}^{N=2,(n)} | \alpha \rangle \\ &= \frac{\bar{\omega}_{q,n}^{(1)}(\alpha)}{2} \hat{\sigma}_z^{(1)} + \frac{\bar{\omega}_{q,n}^{(2)}(\alpha)}{2} \hat{\sigma}_z^{(2)} \\ &\quad + \bar{g}_n(\alpha) (\hat{\sigma}_+^{(1)} \hat{\sigma}_-^{(2)} + \hat{\sigma}_-^{(1)} \hat{\sigma}_+^{(2)}), \end{aligned} \quad (43a)$$

where

$$\bar{\omega}_{q,n}^{(k)}(\alpha) = \omega_q^{(k)} + \chi_n^{(k)} \sum_{k=0}^n \sum_{l=0}^k C_{n,k}^+ s_2(k,l) |\alpha|^l \quad (43b)$$

and

$$\bar{g}_n(\alpha) = \tilde{\chi}_n^{(1,2)} \sum_{k=0}^{n-1} \sum_{l=0}^k C_{n,k}^- s_2(k,l) |\alpha|^l. \quad (43c)$$

We can now tune the effective qubit frequencies and qubit-qubit coupling strength by changing the coherent state amplitude, $|\alpha|$. The effective qubit frequencies follow exactly from the single-qubit-oscillator case in Sec. IIID (see Fig 3). Interestingly, the effective qubit frequencies are polynomial functions of $|\alpha|$ of degree n , whereas the effective qubit-qubit interactions are polynomial functions of degree $n-1$. The tuning of the effective qubit-qubit interaction can be done *in situ* by adjusting the amplitude of the coherent state using a linear drive on the oscillator ($\propto \hat{a}^\dagger \pm \hat{a}$). The tunability and different growth behaviour (depending on the interaction order) of $\bar{g}_n(\alpha)$ will significantly affect the effective two-qubit system since this coupling dictates qubit-qubit transitions such as $|ge\rangle \mapsto |eg\rangle$.

Note that, in principle, we can just easily do the calculations assuming the oscillator to be in some Fock state $|j\rangle$. However, while the preparation of an initial Fock state might be relatively easy using of the two qubits, changing from one Fock state to another while operating the effective two-qubit system will have much more detrimental effects on the two qubits than, e.g., adiabatically changing the coherent state using a linear drive on the oscillator.

V. MULTIPLE OSCILLATORS COUPLED TO A SINGLE QUBIT

We can extend the framework presented in the previous section to the multioscillator scenario. The calculations, straightforwardly, follow from the multiqubit case. We begin with the multiphoton multimode Rabi (MMR) model where we generically assume N oscillators interact with a single qubit via a multiphoton interaction.

We assume that each oscillator can interact with the qubit through a differing interaction order, i.e. the l th oscillator interacts with the qubit through an n_l -photon interaction where generally $n_l \neq n_m$ for $m \neq l$ ³. The MMR Hamiltonian reads

$$\begin{aligned} \hat{H}_{\text{MMR}} &= \sum_k \omega_k \hat{a}_k^\dagger \hat{a}_k + \frac{\omega_q}{2} \hat{\sigma}_z \\ &\quad + \sum_k g_{k,n_k} \hat{\sigma}_x (\hat{a}_k^{\dagger n_k} + \hat{a}_k^{n_k}), \end{aligned} \quad (44)$$

where g_{k,n_k} specifies the k th oscillator's coupling strength to the qubit via an n_k -photon interaction. Similar to

³ As an example, one can think of a qubit simultaneously interacting with two oscillators where one is coupled via a one-photon interaction and the other via a two-photon interaction.

the multiqubit case, when each oscillator is in the n_k -photon JC-RWA regime with respect to its interaction with the qubit. The MMR Hamiltonian can be simplified to the multiphoton multimode Jaynes-Cummings (MMJC) Hamiltonian which reads

$$\begin{aligned} \hat{H}_{\text{MMJC}} = & \sum_k \omega_k \hat{a}_k^\dagger \hat{a}_k + \frac{\omega_q}{2} \hat{\sigma}_z \\ & + \sum_k g_{k,n_k} (\hat{\sigma}_+ \hat{a}_k^{n_k} + \hat{\sigma}_- \hat{a}_k^{\dagger n_k}). \end{aligned} \quad (45)$$

We now proceed to apply the SW transformation in the cases of the RWA and non-RWA regime; the RWA regime takes the MMJC Hamiltonian as the starting point whereas the non-RWA regime considers the MMR Hamiltonian.

Similar to the multiqubit case, the RWA energy scale is defined by $g_{k,n_k} \ll |\Delta_{k,n_k}| \ll \Sigma_{k,n_k}$, where $\Delta_{k,n_k} = \omega_q - n_k \omega_k$ and $\Sigma_{k,n_k} = \omega_q + n_k \omega_k$. We now use the same SW transformation as the multiqubit RWA case with the indices running over the oscillators instead of the qubits;

$$\hat{U}_{\text{Disp,RWA}} = \exp\left(\sum_k \lambda_k \hat{X}_{-,k}\right) \quad (46)$$

where

$$\hat{X}_{\pm,k} = \hat{\sigma}_- \hat{a}_k^{\dagger n_k} \pm \hat{\sigma}_+ \hat{a}_k^{n_k} \quad (47)$$

and $\lambda_k = g_{k,n}/(\omega_q - n_k \omega_r)$. Then, to second order in each λ_k , the multiphoton multioscillator RWA dispersive regime Hamiltonian reads

$$\begin{aligned} \hat{H}_{\text{Disp,RWA}}^{\text{MMO}} = & \hat{U}_{\text{Disp,RWA}}^\dagger \hat{H}_{\text{MMJC}} \hat{U}_{\text{Disp,RWA}} \\ \simeq & \sum_k \hat{H}_{\text{Disp,RWA}}^k \\ & + \sum_{l>k} \tilde{\chi}_{k,l} \hat{\sigma}_z (\hat{a}_k^{\dagger n_k} \hat{a}_l^{n_l} + \hat{a}_k^{n_k} \hat{a}_l^{\dagger n_l}), \end{aligned} \quad (48)$$

where $\hat{H}_{\text{Disp,RWA}}^k$ is the k th oscillator RWA dispersive Hamiltonian of Eq. (27) with n_k replacing n . Here, a qubit-conditional multiphoton n_k -to- n_l -downconversion interaction emerges.

Similarly to the multiqubit case, the non-RWA extended generator can also be generalized from the multiqubit case where it runs over oscillator indices;

$$\hat{Y}_{\pm,k} = \hat{\sigma}_- \hat{a}_k^{n_k} \pm \hat{\sigma}_+ \hat{a}_k^{\dagger n_k}. \quad (49)$$

Thus, the non-RWA transformation becomes

$$\hat{U}_{\text{Disp}} = \exp\left(\sum_k \lambda_k \hat{X}_{-,k} + \sum_k \bar{\lambda}_k \hat{Y}_{-,k}\right) \quad (50)$$

where $\bar{\lambda}_k = g_{k,n}/(\omega_q + n_k \omega_r)$. Then, to second order in all perturbation parameters, the non-RWA multiphoton

multimode dispersive Hamiltonian is

$$\begin{aligned} \hat{H}_{\text{Disp}}^{\text{MMO}} = & \hat{U}_{\text{Disp}}^\dagger \hat{H}_{\text{MMR}} \hat{U}_{\text{Disp}} \\ \simeq & \sum_k \hat{H}_{\text{Disp}}^k \\ & + \sum_{l>k} \frac{(\tilde{\chi}_{k,l} + \tilde{\xi}_{k,l})}{2} \hat{\sigma}_z (\hat{a}_k^{\dagger n_k} + \hat{a}_k^{n_k}) (\hat{a}_l^{\dagger n_l} + \hat{a}_l^{n_l}), \end{aligned} \quad (51)$$

where \hat{H}_{Disp}^k is the k th oscillator non-RWA dispersive Hamiltonian of Eq. (32) with n_k replacing n . In this case, the qubit-conditional interaction arising comprises both excitation-perserving and non-perserving terms.

It is interesting to contrast the multiqubit and multimode cases. In the multiqubit case, the mediated qubit-qubit interaction is photon-number dependent and involves sums over the powers of the photon number operators, whereas in the multimode case, the mediated oscillator-oscillator interaction depends on $\hat{\sigma}_z$ and not higher powers of $\hat{\sigma}_z$ ⁴. The reason for the summation over photon-number powers in the multiqubit scenario is due to the higher-order commutators, e.g. $[\hat{a}^n, \hat{a}^{\dagger n}]$, attached to the effective qubit-qubit interaction term in the perturbative expansion. The resulting qubit-conditional interactions can be utilized for creating interesting non-Gaussian states, qubit-controlled interferometry and multiphoton down-conversion [52]. Additionally, these interactions can be leveraged for faster multimode unitary synthesis over the total Hilbert space [22, 61]. Using similar parameters for the superconducting circuits example in Sec III D, we can find estimates for these mediated interactions to be on the order of a few MHz.

VI. SUMMARY AND CONCLUSIONS

Typical SW-type perturbation theory transformations are used to decouple low-energy and high-energy subspaces; this allows us to obtain an effective description of a complicated many-body system within its low-energy subspaces [53]. The presented generalization provides an accurate description for the lower-energy states, and the accuracy becomes ever-vanishing for higher-energy states, as expected from a low-energy effective description of the system. In the usual linear interaction qubit-oscillator dispersive regime, the accuracy is commonly bounded by a critical photon number, $n_c = g^2/4\Delta^2$, which signifies the growing deviation between the perturbative and full system Hamiltonians for oscillator photon occupation numbers beyond it. A general bound on the

⁴ If it were the case, summing over higher powers of $\hat{\sigma}_z$ would result in an additional unconditional interaction since $\hat{\sigma}_z^k = \hat{\mathbb{I}}$ for even k and stronger conditional interactions since $\hat{\sigma}_z^k = \hat{\sigma}_z$ for odd k .

spectra to match this new notion of critical photon number is difficult to obtain for the multiphoton dispersive regime as it depends on multiple parameters such as n , g_n , and Δ_n . In practice, such a bounding parameter will depend on the additional imperfections and spurious effects of a given implementation choice.

A surprising find is the non-RWA approximation is less accurate than its RWA counterpart. This suggests that the role of the counter-rotating terms is not accounted for by a simple extension of the SW transformation generators. Unlike the dispersive regime of the linear interaction, we find the multiphoton non-RWA dispersive regime to not provide accurate descriptions of the system at larger coupling strengths.

In the generalized case of multiple qubits nonlinearly coupled to a shared oscillator, we found similar trends to the single qubit-oscillator case with some differences due to the cooperative effects. Generally, the perturbative spectra presented provide an accurate description for the multiqubit case when the qubits' couplings are in the individual qubit-oscillator regime of validity. When one of the qubits is outside its perturbative regime of validity, the perturbative descriptions are applicable for a much smaller range of parameters. The second key difference is the emergence of a photon-number-dependent qubit-qubit interaction. Incidentally, this allows for an effective tuning of the two-qubit system parameters. The state of the oscillator can then be used to tune the effective multiqubit system parameters.

Furthermore, we highlighted important experimental signatures that distinguish the different dispersive interaction orders. In the single qubit-oscillator case, the effective dressed qubit frequency when the oscillator is populated with a coherent state. We found the shift in dressed frequency to be a polynomial function of the coherent state amplitude with order n . In the case of multiple qubits, the tunable photon-number dependent qubit-qubit interaction, which also happens to be a polynomial but of degree $n - 1$, serves as a signature since its strength can significantly alter the qubits' transitions, e.g. $|ge\rangle \mapsto |eg\rangle$.

In Sec. V, we further extended the multiphoton dispersive regime to the converse multipartite scenario where N oscillators are nonlinearly coupled to a single qubit. Here, we find qubit-conditional oscillator-oscillator nonlinear interactions. This can be of great interest for bosonically-encoded quantum computation research. The interest stems from the nonlinear terms being useful for control and readout since in this scenario, one relies on a qubit to control and readout the logical oscillator modes.

In summary, we developed a generalized SW perturbation theory for the dispersive regime of a qubit-oscillator system interacting through an n -photon interaction. We considered a generalization of the one-photon RWA and non-RWA dispersive-regime SW transformations, and we examined the accuracy of their predictions (to second order in the perturbation parameters) compared to numerical (and semi-analytical) results. This framework was

then generalized to two multipartite scenarios, multiple qubits coupled to a shared oscillator, and multiple oscillators coupled to a shared qubit. The multiphoton SW transformation presented here and its multipartite generalizations are important in their relation to the rising number of applications of collective cooperative phenomena for sensing [62], unitary synthesis and universal control [22, 61], and nonlinear interferometry and multiphoton spontaneous parametric down-conversion [52]. We believe the work presented here can serve as a guide for designing experimental implementations exploiting the desired effects of dispersive multiphoton qubit-oscillator interactions.

ACKNOWLEDGMENTS

M.A. was supported by the Institute for Quantum Computing (IQC) through funding provided by Transformative Quantum Technologies (TQT). S.A. was supported by Japan's Ministry of Education, Culture, Sports, Science and Technology's Quantum Leap Flagship Program Grant No. JPMXS0120319794.

Appendix A: Combinatorial aspects of multiphoton perturbation theory

The perturbative RWA and non-RWA expansions used in the main text rely on the commutators arising from the first and second order BCH expansion terms. These terms rely on the commutators $[\hat{X}_{+n}, \hat{X}_{-n}]$, $[\hat{Y}_{+n}, \hat{X}_{-n}]$, $[\hat{X}_{+n}, \hat{Y}_{-n}]$, and $[\hat{Y}_{+n}, \hat{Y}_{-n}]$. In this appendix, we explicitly express these commutators in the diagonal form shown in the main text.

We begin by showing all the steps involved in evaluating $[\hat{X}_{+n}, \hat{X}_{-n}]$ from which $[\hat{Y}_{+n}, \hat{Y}_{-n}]$ immediately follows; $[\hat{X}_{+n}, \hat{Y}_{-n}]$ and $[\hat{Y}_{+n}, \hat{X}_{-n}]$ can be immediately evaluated and both are equal to $\hat{\sigma}_z(\hat{a}^{\dagger 2n} - \hat{a}^{2n})$. The commutator reads as

$$\begin{aligned} [\hat{X}_{+n}, \hat{X}_{-n}] &= [\hat{\sigma}_- \hat{a}^{\dagger n} + \hat{\sigma}_+ \hat{a}^n, \hat{\sigma}_- \hat{a}^{\dagger n} - \hat{\sigma}_+ \hat{a}^n] \\ &= \hat{\sigma}_z \{ \hat{a}^n, \hat{a}^{\dagger n} \} + [\hat{a}^n, \hat{a}^{\dagger n}], \end{aligned} \quad (\text{A1})$$

where $\{, \}$ is the anti-commutator. We now apply the normal-ordering procedure, $\mathcal{N}[\dots]$, that allows us to rewrite $\hat{a}^n \hat{a}^{\dagger n}$ as [63]

$$\hat{a}^n \hat{a}^{\dagger n} = \mathcal{N}[\hat{a}^n \hat{a}^{\dagger n}] = \sum_{k=0}^n \binom{n}{k} n^k \hat{a}^{\dagger n-k} \hat{a}^{n-k}, \quad (\text{A2})$$

where $\binom{n}{k} = n!/(k!(n-k)!)$ and $n^{\underline{k}} = n(n-1)\dots(n-k+1)$ is the falling factorial with the convention $n^{\underline{0}} = 1$. Next, we use the identity [59],

$$\hat{a}^{\dagger n} \hat{a}^n = \sum_{k=0}^n s_1(n, k) (\hat{a}^{\dagger} \hat{a})^k, \quad (\text{A3})$$

to obtain a power series in the photon-number operator. Here, we recall that $s_1(n, k)$ are Stirling numbers of the first kind. Thus, we readily have the desired expression for $\hat{a}^{\dagger n} \hat{a}^n$, but we must further simplify the term $\hat{a}^n \hat{a}^{\dagger n}$. It can be shown using some combinatorial tricks that [64]

$$\begin{aligned} \hat{a}^n \hat{a}^{\dagger n} &= \sum_{k=0}^n \binom{n}{k} n^k \hat{a}^{\dagger n-k} \hat{a}^{n-k} \\ &= \sum_{k=0}^n (-1)^{(n+k)} s_1(n+1, k+1) (\hat{a}^{\dagger} \hat{a})^k. \end{aligned} \quad (\text{A4})$$

Thus, we may now express the commutator $[\hat{X}_{+n}, \hat{X}_{-n}]$ in diagonal form as

$$\begin{aligned} [\hat{X}_{+n}, \hat{X}_{-n}] &= \hat{\sigma}_z \{ \hat{a}^n, \hat{a}^{\dagger n} \} + [\hat{a}^n, \hat{a}^{\dagger n}] \\ &= \hat{\sigma}_z \sum_{k=0}^n C_{n,k}^+ (\hat{a}^{\dagger} \hat{a})^k + \sum_{k=0}^{n-1} C_{n,k}^- (\hat{a}^{\dagger} \hat{a})^k \end{aligned} \quad (\text{A5})$$

where

$$C_{n,k}^{\pm} = (-1)^{n+k} s_1(n+1, k+1) \pm s_1(n, k). \quad (\text{A6})$$

The qubit-state-independent sum terminates at $k = n-1$ because $C_{n,n}^- = 0$. We can now simply reuse these results for the other commutator, $[\hat{Y}_{+n}, \hat{Y}_{-n}]$:

$$\begin{aligned} [\hat{Y}_{+n}, \hat{Y}_{-n}] &= [\hat{\sigma}_- \hat{a}^n + \hat{\sigma}_+ \hat{a}^{\dagger n}, \hat{\sigma}_- \hat{a}^n - \hat{\sigma}_+ \hat{a}^{\dagger n}] \\ &= \hat{\sigma}_z \{ \hat{a}^n, \hat{a}^{\dagger n} \} - [\hat{a}^n, \hat{a}^{\dagger n}] \\ &= \hat{\sigma}_z \sum_{k=0}^n C_{n,k}^+ (\hat{a}^{\dagger} \hat{a})^k - \sum_{k=0}^{n-1} C_{n,k}^- (\hat{a}^{\dagger} \hat{a})^k. \end{aligned} \quad (\text{A7})$$

This last equation explains why the non-RWA qubit-state-independent oscillator Kerr terms come with a minus sign ($-\xi_n$).

We may now find the second order RWA and non-RWA dispersive Hamiltonians presented in the main text. The BCH expansion truncated at second order for the RWA Hamiltonian reads

$$\begin{aligned} \hat{H}_{\text{Disp,RWA}}^{(n),2} &= \hat{H}_{n\text{-JC}} + \lambda_n [\hat{H}_{n\text{-JC}}, \hat{X}_{-n}] \\ &\quad + \frac{\lambda_n^2}{2} [[\hat{H}_{n\text{-JC}}, \hat{X}_{-n}], \hat{X}_{-n}] \\ &= \hat{H}_{n\text{-JC}} - \Delta_n \lambda_n \hat{X}_{-n} \\ &\quad + \left(g_n \lambda_n - \frac{\Delta_n \lambda_n^2}{2} \right) [\hat{X}_{+n}, \hat{X}_{-n}] \\ &\quad + \frac{g_n \lambda_n^2}{2} [[\hat{X}_{+n}, \hat{X}_{-n}], \hat{X}_{-n}] \\ &= \omega_o \hat{a}^{\dagger} \hat{a} + \frac{\omega_q}{2} \hat{\sigma}_z + \frac{\chi_n}{2} \sum_{k=0}^n C_{n,k}^+ \hat{\sigma}_z (\hat{a}^{\dagger} \hat{a})^k \\ &\quad + \frac{\chi_n}{2} \sum_{k=1}^{n-1} C_{n,k}^- (\hat{a}^{\dagger} \hat{a})^k \\ &\quad + \frac{g_n^3}{2\Delta_n} [[\hat{X}_{+n}, \hat{X}_{-n}], \hat{X}_{-n}], \end{aligned} \quad (\text{A8})$$

where we used $[\hat{H}_{n\text{-JC}}, \hat{X}_{-n}] = -\Delta_n \hat{X}_{-n} + g_n [\hat{X}_{+n}, \hat{X}_{-n}]$. The last term is on the order of λ_n^3 and, thus, neglected from Hamiltonian of Eq. (27) presented in the main text. A similar calculation for the non-RWA Hamiltonian yields

$$\begin{aligned} \hat{H}_{\text{Disp}}^{(n),2} &= \hat{H}_{n\text{-R}} + \lambda_n [\hat{H}_{n\text{-R}}, \hat{X}_{-n}] + \bar{\lambda}_n [\hat{H}_{n\text{-R}}, \hat{Y}_{-n}] + \frac{\lambda_n^2}{2} [[\hat{H}_{n\text{-R}}, \hat{X}_{-n}], \hat{X}_{-n}] + \frac{\bar{\lambda}_n^2}{2} [[\hat{H}_{n\text{-R}}, \hat{Y}_{-n}], \hat{Y}_{-n}] \\ &\quad + \frac{\lambda_n \bar{\lambda}_n}{2} [[\hat{H}_{n\text{-R}}, \hat{X}_{-n}], \hat{Y}_{-n}] + \frac{\bar{\lambda}_n \lambda_n}{2} [[\hat{H}_{n\text{-R}}, \hat{Y}_{-n}], \hat{X}_{-n}] \\ &= \hat{H}_{n\text{-R}} - \Delta_n \lambda_n \hat{X}_{-n} + \left(g_n \lambda_n - \frac{\Sigma_n \lambda_n \bar{\lambda}_n}{2} \right) [\hat{Y}_{+n}, \hat{X}_{-n}] + \left(g_n \lambda_n - \frac{-\Delta_n \lambda_n^2}{2} \right) [\hat{X}_{+n}, \hat{X}_{-n}] - \Sigma_n \bar{\lambda}_n \hat{Y}_{-n} \\ &\quad + \left(g_n \bar{\lambda}_n - \frac{\Sigma_n \bar{\lambda}_n^2}{2} \right) [\hat{Y}_{+n}, \hat{Y}_{-n}] + \left(g_n \bar{\lambda}_n - \frac{\Delta_n \bar{\lambda}_n \lambda_n}{2} \right) [\hat{X}_{+n}, \hat{Y}_{-n}] \\ &\quad + \frac{g_n}{2} \left(\lambda_n^2 ([[\hat{X}_{+n}, \hat{X}_{-n}], \hat{X}_{-n}] + [[\hat{Y}_{+n}, \hat{X}_{-n}], \hat{X}_{-n}]) + \bar{\lambda}_n^2 ([[\hat{X}_{+n}, \hat{Y}_{-n}], \hat{Y}_{-n}] + [[\hat{Y}_{+n}, \hat{Y}_{-n}], \hat{Y}_{-n}]) \right. \\ &\quad \left. + \lambda_n \bar{\lambda}_n ([[\hat{X}_{+n}, \hat{Y}_{-n}], \hat{X}_{-n}] + [[\hat{Y}_{+n}, \hat{X}_{-n}], \hat{Y}_{-n}]) + [[\hat{X}_{+n}, \hat{X}_{-n}], \hat{Y}_{-n}] + [[\hat{Y}_{+n}, \hat{Y}_{-n}], \hat{X}_{-n}] \right) \end{aligned}$$

$$\begin{aligned}
&= \omega_o \hat{a}^\dagger \hat{a} + \frac{\omega_q}{2} \hat{\sigma}_z + \frac{(\chi_n + \xi_n)}{2} \sum_{k=0}^n C_{n,k}^+ \hat{\sigma}_z (\hat{a}^\dagger \hat{a})^k + \frac{(\chi_n - \xi_n)}{2} \sum_{k=1}^{n-1} C_{n,k}^- (\hat{a}^\dagger \hat{a})^k + \frac{(\chi_n + \xi_n)}{2} \hat{\sigma}_z (\hat{a}^{\dagger 2n} + \hat{a}^{2n}) \\
&+ \frac{g_n}{2} \left(\lambda_n^2 ([[\hat{X}_{+n}, \hat{X}_{-n}], \hat{X}_{-n}] + [[\hat{Y}_{+n}, \hat{X}_{-n}], \hat{X}_{-n}]) + \bar{\lambda}_n^2 ([[\hat{X}_{+n}, \hat{Y}_{-n}], \hat{Y}_{-n}] + [[\hat{Y}_{+n}, \hat{Y}_{-n}], \hat{Y}_{-n}]) \right. \\
&\left. + \lambda_n \bar{\lambda}_n ([[\hat{X}_{+n}, \hat{Y}_{-n}], \hat{X}_{-n}] + [[\hat{Y}_{+n}, \hat{X}_{-n}], \hat{Y}_{-n}] + [[\hat{X}_{+n}, \hat{X}_{-n}], \hat{Y}_{-n}] + [[\hat{Y}_{+n}, \hat{Y}_{-n}], \hat{X}_{-n}]) \right), \tag{A9}
\end{aligned}$$

where we used $[\hat{H}_{n-R}, \hat{X}_{-n}] = -\Delta_n \hat{X}_{+n} + g_n [\hat{Y}_{+n}, \hat{X}_{-n}] + g_n [\hat{X}_{+n}, \hat{X}_{-n}]$ and $[\hat{H}_{n-R}, \hat{X}_{-n}] =$

$-\Sigma_n \hat{Y}_{+n} + g_n [\hat{Y}_{+n}, \hat{Y}_{-n}] + g_n [\hat{X}_{+n}, \hat{Y}_{-n}]$. The last eight terms comprising nested commutators are of third order in λ_n and $\bar{\lambda}_n$, and, thus, are not included in the non-RWA Hamiltonian of Eq. (32).

-
- [1] E. Jaynes and F. Cummings, Proceedings of the IEEE **51**, 89 (1963).
- [2] I. I. Rabi, Phys. Rev. **49**, 324 (1936).
- [3] I. I. Rabi, Phys. Rev. **51**, 652 (1937).
- [4] S. Haroche and J.-M. Raimond, *Exploring the Quantum: Atoms, Cavities, and Photons* (Oxford University Press, 2006).
- [5] A. Blais, A. L. Grimsmo, S. M. Girvin, and A. Wallraff, Rev. Mod. Phys. **93**, 025005 (2021).
- [6] D. Leibfried, R. Blatt, C. Monroe, and D. Wineland, Rev. Mod. Phys. **75**, 281 (2003).
- [7] B. Buck and C. Sukumar, Physics Letters A **81**, 132 (1981).
- [8] S. Singh, Phys. Rev. A **25**, 3206 (1982).
- [9] V. Bužek, Phys. Rev. A **39**, 3196 (1989).
- [10] M. S. Abdalla, S. S. Hassan, and A. S. F. Obada, Phys. Rev. A **34**, 4869 (1986).
- [11] E. I. Aliskenderov, K. A. Rustamov, A. S. Shumovsky, and T. Quang, Journal of Physics A: Mathematical and General **20**, 6265 (1987).
- [12] I. Ashraf, J. Gea-Banacloche, and M. S. Zubairy, Phys. Rev. A **42**, 6704 (1990).
- [13] J. Larson and T. Mavrogordatos, *The Jaynes–Cummings Model and Its Descendants*, 2053-2563 (IOP Publishing, 2021).
- [14] K. M. Ng, C. F. Lo, and K. L. Liu, The European Physical Journal D - Atomic, Molecular, Optical and Plasma Physics **6**, 119 (1999).
- [15] C. Emary and R. F. Bishop, Journal of Physics A: Mathematical and General **35**, 8231 (2002).
- [16] I. Travènc, Phys. Rev. A **85**, 043805 (2012).
- [17] L. Duan, Y.-F. Xie, D. Braak, and Q.-H. Chen, Journal of Physics A: Mathematical and Theoretical **49**, 464002 (2016).
- [18] D. Braak, Phys. Rev. Lett. **107**, 100401 (2011).
- [19] Q.-H. Chen, C. Wang, S. He, T. Liu, and K.-L. Wang, Phys. Rev. A **86**, 023822 (2012).
- [20] S. Cui, J.-P. Cao, H. Fan, and L. Amico, Journal of Physics A: Mathematical and Theoretical **50**, 204001 (2017).
- [21] M. Drechsler, M. Belén Farías, N. Freitas, C. T. Schmiegelow, and J. P. Paz, Phys. Rev. A **101**, 052331 (2020).
- [22] M. Ayyash, X. Xu, S. Ashhab, and M. Mariani, Phys. Rev. A **104**, 003700 (2024).
- [23] S. Saner, O. Băzăvan, D. J. Webb, G. Araneda, D. M. Lucas, C. J. Ballance, and R. Srinivas, Generating arbitrary superpositions of nonclassical quantum harmonic oscillator states (2024), arXiv:2409.03482 [quant-ph].
- [24] S. Felicetti, D. Z. Rossatto, E. Rico, E. Solano, and P. Forn-Díaz, Phys. Rev. A **97**, 013851 (2018).
- [25] S. Felicetti, M.-J. Hwang, and A. Le Boité, Phys. Rev. A **98**, 053859 (2018).
- [26] F. Zou, X.-Y. Zhang, X.-W. Xu, J.-F. Huang, and J.-Q. Liao, Phys. Rev. A **102**, 053710 (2020).
- [27] R. Puebla, M.-J. Hwang, J. Casanova, and M. B. Plenio, Phys. Rev. A **95**, 063844 (2017).
- [28] A. Blais, J. Gambetta, A. Wallraff, D. I. Schuster, S. M. Girvin, M. H. Devoret, and R. J. Schoelkopf, Phys. Rev. A **75**, 032329 (2007).
- [29] D. Zueco, G. M. Reuther, S. Kohler, and P. Hänggi, Phys. Rev. A **80**, 033846 (2009).
- [30] F. Beaudoin, J. M. Gambetta, and A. Blais, Phys. Rev. A **84**, 043832 (2011).
- [31] J. R. Schrieffer and P. A. Wolff, Phys. Rev. **149**, 491 (1966).
- [32] M. Boissonneault, J. M. Gambetta, and A. Blais, Phys. Rev. Lett. **105**, 100504 (2010).
- [33] P. Forn-Díaz, J. Lisenfeld, D. Marcos, J. J. García-Ripoll, E. Solano, C. J. P. M. Harmans, and J. E. Mooij, Phys. Rev. Lett. **105**, 237001 (2010).
- [34] T. Niemczyk, F. Deppe, H. Huebl, E. P. Menzel, F. Hocke, M. J. Schwarz, J. J. Garcia-Ripoll, D. Zueco, T. Hümmer, E. Solano, A. Marx, and R. Gross, Nature Physics **6**, 772 (2010).
- [35] F. Yoshihara, T. Fuse, S. Ashhab, K. Kakuyanagi, S. Saito, and K. Semba, Nature Physics **13**, 44 (2017).
- [36] C. Joshi, E. K. Irish, and T. P. Spiller, Scientific Reports **7**, 45587 (2017).
- [37] R. H. Dicke, Phys. Rev. **93**, 99 (1954).
- [38] K. Hepp and E. H. Lieb, Annals of Physics **76**, 360 (1973).
- [39] Y. K. Wang and F. T. Hioe, Phys. Rev. A **7**, 831 (1973).
- [40] M. Tavis and F. W. Cummings, Phys. Rev. **170**, 379 (1968).
- [41] K. Kakuyanagi, Y. Matsuzaki, C. Déprez, H. Toida, K. Semba, H. Yamaguchi, W. J. Munro, and S. Saito, Phys. Rev. Lett. **117**, 210503 (2016).

- [42] W.-L. Ma, S. Puri, R. J. Schoelkopf, M. H. Devoret, S. Girvin, and L. Jiang, *Science Bulletin* **66**, 1789 (2021).
- [43] Y. Liu, S. Singh, K. C. Smith, E. Crane, J. M. Martyn, A. Eickbusch, A. Schuckert, R. D. Li, J. Sinanan-Singh, M. B. Soley, T. Tsunoda, I. L. Chuang, N. Wiebe, and S. M. Girvin, Hybrid oscillator-qubit quantum processors: Instruction set architectures, abstract machine models, and applications (2024), arXiv:2407.10381 [quant-ph].
- [44] T. Niemczyk, F. Deppe, H. Huebl, E. P. Menzel, F. Hocke, M. J. Schwarz, J. J. Garcia-Ripoll, D. Zueco, T. Hümmer, E. Solano, A. Marx, and R. Gross, *Nature Physics* **6**, 772 (2010).
- [45] N. M. Sundaresan, Y. Liu, D. Sadri, L. J. Szócs, D. L. Underwood, M. Malekakhlagh, H. E. Türeci, and A. A. Houck, *Phys. Rev. X* **5**, 021035 (2015).
- [46] Z. Ao, S. Ashhab, F. Yoshihara, T. Fuse, K. Kakuyanagi, S. Saito, T. Aoki, and K. Semba, *Scientific Reports* **13**, 11340 (2023).
- [47] M. Mariantoni, F. Deppe, A. Marx, R. Gross, F. K. Wilhelm, and E. Solano, *Phys. Rev. B* **78**, 104508 (2008).
- [48] B. J. Chapman, S. J. de Graaf, S. H. Xue, Y. Zhang, J. Teoh, J. C. Curtis, T. Tsunoda, A. Eickbusch, A. P. Read, A. Koottandavida, S. O. Mundhada, L. Frunzio, M. Devoret, S. Girvin, and R. Schoelkopf, *PRX Quantum* **4**, 020355 (2023).
- [49] N. C. Menicucci, P. van Loock, M. Gu, C. Weedbrook, T. C. Ralph, and M. A. Nielsen, *Phys. Rev. Lett.* **97**, 110501 (2006).
- [50] R. J. A. Rico, F. H. Maldonado-Villamizar, and B. M. Rodriguez-Lara, *Phys. Rev. A* **101**, 063825 (2020).
- [51] D. Braak, The k -photon quantum rabi model (2025), arXiv:2401.02370 [quant-ph].
- [52] C. W. S. Chang, C. Sabín, P. Forn-Díaz, F. Quijandría, A. M. Vadiraj, I. Nsanzineza, G. Johansson, and C. M. Wilson, *Phys. Rev. X* **10**, 011011 (2020).
- [53] S. Bravyi, D. P. DiVincenzo, and D. Loss, *Annals of Physics* **326**, 2793 (2011).
- [54] M. Boissonneault, J. M. Gambetta, and A. Blais, *Phys. Rev. Lett.* **105**, 100504 (2010).
- [55] A. Miranowicz, M. Paprzycka, Y.-x. Liu, J. c. v. Bajer, and F. Nori, *Phys. Rev. A* **87**, 023809 (2013).
- [56] B. Yurke and D. Stoler, *Phys. Rev. Lett.* **57**, 13 (1986).
- [57] F. Yoshihara, T. Fuse, S. Ashhab, K. Kakuyanagi, S. Saito, and K. Semba, *Phys. Rev. A* **95**, 053824 (2017).
- [58] D. Z. Rossatto, C. J. Villas-Bôas, M. Sanz, and E. Solano, *Phys. Rev. A* **96**, 013849 (2017).
- [59] J. Katriel, *Physics Letters A* **273**, 159 (2000).
- [60] S. Ashhab and K. Semba, *Phys. Rev. A* **95**, 053833 (2017).
- [61] A. Eickbusch, V. Sivak, A. Z. Ding, S. S. Elder, S. R. Jha, J. Venkatraman, B. Royer, S. M. Girvin, R. J. Schoelkopf, and M. H. Devoret, *Nature Physics* **18**, 1464 (2022).
- [62] M. Koppenhöfer, P. Groszkowski, H.-K. Lau, and A. Clerk, *PRX Quantum* **3**, 030330 (2022).
- [63] P. Blasiak, A. Horzela, K. A. Penson, A. I. Solomon, and G. H. E. Duchamp, *American Journal of Physics* **75**, 639 (2007), https://pubs.aip.org/aapt/ajp/article-pdf/75/7/639/13083703/639_1_online.pdf.
- [64] P. Blasiak, K. A. Penson, and A. I. Solomon, *Annals of Combinatorics* **7**, 127 (2003).